GEOLOGICA CARPATHICA, OCTOBER 2014, 65, 5, 329–338 doi: 10.2478/geoca-2014-0023

Provenance of Permian Malužiná Formation sandstones (Hronicum, Western Carpathians): evidence from monazite geochronology

ANNA VOZÁROVÁ[1], PATRIK KONEČNÝ[2], MAREK VĎAČNÝ[3], JOZEF VOZÁR[4] and KATARÍNA ŠARINOVÁ[1]

[1]Department of Mineralogy and Petrology, Faculty of Natural Sciences, Comenius University in Bratislava, Mlynská dolina G, 842 15 Bratislava, Slovak Republic; vozarova@fns.uniba.sk; sarinova@fns.uniba.sk
[2]State Geological Institute of Dionýz Štúr, Mlynská dolina 1, 817 04 Bratislava, Slovak Republic; konecny.patrik@geology.sk
[3]Geological Institute, Slovak Academy of Sciences; Branch: Ďumbierska 1, 974 01 Banská Bystrica, Slovak Republic; vdacny@savbb.sk
[4]Geological Institute, Slovak Academy of Sciences, Dúbravská cesta 9, P.O. Box 106, 840 05 Bratislava, Slovak Republic; jozef.vozar@savba.sk

(Manuscript received March 10, 2014; accepted in revised form October 7, 2014)

Abstract: The Permian Malužiná Formation and the Pennsylvanian Nižná Boca Formation are Upper Paleozoic volcano-sedimentary complexes in the Hronicum nappe system. Sandstones, shales and conglomerates are the dominant lithological members of the Malužiná Formation sequence. Detrital monazites were analysed by electron microprobe, to obtain Th-U-Pb ages of the source areas. The majority of detrital monazites showed Devonian-Mississippian ages, ranging from 330 to 380 Ma with a weighted average of 351 ± 3.3 (2σ), that correspond well with the main phase of arc-related magmatic activity in the Western Carpathians. Only a small portion of detrital monazites displayed Permian ages in the range of 250–280 Ma, with a significant maximum around 255 Ma. The weighted average corresponds to 255 ± 6.2 Ma. These monazites may have been partially derived from the synsedimentary acid volcanism that was situated on the margins of the original depositional basin. However, some of the Triassic ages (230–240 Ma), reflect, most likely, the genetic relationship with the overheating connected with Permian and subsequent Triassic extensional regime. Detrital monazite ages document the Variscan age of the source area and also reflect a gradual development of the Hronicum terrestrial rift, accompanied by the heterogeneous cooling of the lithosphere.

Key words: electron microprobe monazite dating, provenance, Permian sandstones, Hronicum, Western Carpathians.

Introduction

Detrital monazite is a common component of siliciclastic sediments and sedimentary rocks, where it is concentrated in heavy mineral assemblages. Monazite is generally stable during sedimentary and diagenetic processes (Morton & Hallsworth 1999), although alteration by the low-temperature brines associated with uranium mineralization has also been reported (Mathieu et al. 2001). Detrital monazites are believed to be unstable in the early stage of regional metamorphism, however, the relics of detrital monazite grains have been reported from greenschist facies (e.g. Rubato et al. 2001; Wing et al. 2003; Rasmussen & Muhling 2009) and even in amphibolite facies rock complexes (e.g. Williams 2001; Krenn et al. 2008). Therefore, chemical electron microprobe dating of detrital monazite also has a great potential to obtain reliable constraints useful for dating source areas and further characteristics of provenance.

The present study reports the first detrital monazite ages from the Permian sandstones of the Hronicum Unit, obtained from the six samples cropping out in the Malé Karpaty Mts. The aim of this study is to contribute to a better understanding of the link between source areas of the Permian Hronicum sedimentary rocks, as well as the tectono-metamorphic evolution of the Western Carpathian Variscan mobile belt.

Geological setting

The Late Paleozoic volcanic and sedimentary rocks represented by the Ipoltica Group form the basal part of the multinappe Hronicum Unit in the whole area of the Western Carpathians. This Upper Paleozoic volcano-sedimentary sequence is distributed in almost all Western Carpathians mountain ranges. Specifically, it occurs in the Malé Karpaty Mts, in the central part of Slovakia, in the Nízke Tatry Mts and Kozie chrbty hills (dominant distribution), in the basement of the Tertiary of the Popradská and Hornádska kotlina Depressions, as well as in the Levočské vrchy hills, the Branisko Mts (fragmentary occurrences), and in the area of the tectonic contact of the Gemericum and Veporicum Units in the Čierna Hora Mts. On the basis of the most completely preserved sedimentary successions on the northern slopes of the Nízke Tatry Mts, the Ipoltica Group was defined as the lithostratigraphic unit composed of two formations — the Nižná Boca (Pennsylvanian) and the Malužiná (Permian) Formations (Vozárová & Vozár 1981).

In the Malé Karpaty Mts, the rock complexes of the Ipoltica Group emerge in the basal part of the lower (Šturec) nappe of the Hronicum. Their occurrences extend in a wide belt (1.5–2.5 km), from the villages of Smolenice and Lošonec in the NE to the area that is S of Sološnica in the W (Fig. 1). The

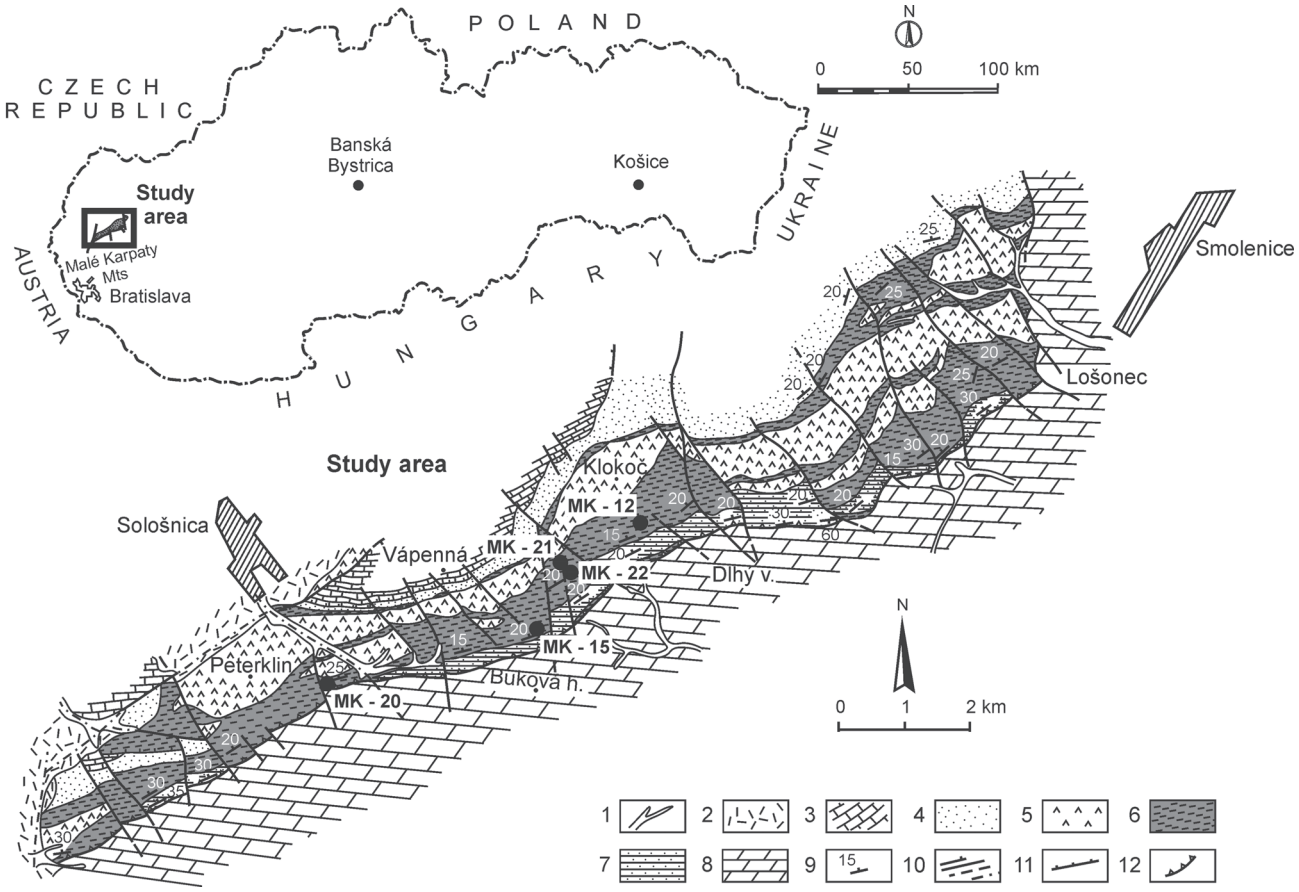

Fig. 1. Map of Slovakia showing the location of the study area (marked by a rectangle). Details of the studied area are depicted below the map of Slovakia in a form of a simplified geological map of the Late Paleozoic rocks of the Hronic Unit in the Malé Karpaty Mts (after Vozárová & Vozár 1988). This geological map also shows five sampling sites. **1** — Quaternary sediments, **2** — Tertiary sediments. **Hronic Unit–Šturec Nappe:** 3 — Middle and Upper Triassic — carbonates, undivided; 4 — Lower Triassic — quartz sandstones, shales; 5 — Permian — andesites, basalts and volcanoclastics (Malužiná Formation); 6 — Permian — conglomerates, sandstones, shales with volcanogenic material admixture (Malužiná Formation); 7 — Uppermost Pennsylvanian — grey conglomerates, sandstones, shales (Nižná Boca Formation). **Krížna Nappe:** 8 — Mesozoic, undivided. **Others:** 9 — foliation cleavage, 10 — faults, 11 — overthrusts, 12 — overthrust line of nappes.

Mesozoic sequences of the Vysoká Nappe of the Fatricum Unit form tectonic basement of the Hronicum in the whole area of the Ipoltica Group. Both cover nappe units, the Hronicum and Fatricum, have been transported over the underlying Tatricum Unit during the Middle Cretaceous detachment and nappe stacking. The possible emplacement mechanism was studied by Prokešová et al. (2012 and references therein). Basal parts of the Hronicum Unit, represented especially by the Nižná Boca Formation (NBF), are markedly tectonically reduced in the Malé Karpaty Mts. Due to this, only the sediments of the Malužiná Formation (MF) were researched in the present study. The MF mineralogical immature sediments examined are covered by the Lower Triassic quartzose sandstones.

***Lithology*:** The MF sediments are formed by a relatively monotonous, markedly cyclically arranged, varicoloured complex of siliciclastic sediments that are genetically associated with a continental alluvial-lacustrine system deposited in arid/semiarid climatic conditions. In the studied area, varicoloured sandstones prevail and are associated with shales and fine-grained conglomerates. Mineral composition of the sandstones corresponds to subarkoses, arkoses and arkosic greywackes, depending upon the type of sedimentary environment in which they occur. Channel facies are structurally more mature, composed of orthoconglomerates and sandstones with the grain-supported fabric. These sandstones can be classified as arkoses and less frequently as subarkoses, either with siliceous or calciferous cement. The carbonate cement signalizes periods of more intensive aridization of the climate. River-floodplain facies are represented by structurally immature red arkosic greywackes, with a higher content of the primary matrix. The MF is characterized by the presence of basalts and basaltic andesites of a continental tholeiite type, which are delimited into two eruption phases in the Nízke Tatry Mts (Vozár 1977, 1997; Dostal et al. 2003). In the area of the MF in the Malé Karpaty Mts, besides the characteristic red-beds sediments, only the continental tholeiites of the second volcanic eruption phase are preserved.

Sample characteristics

Detrital monazites were studied in six sandstone samples (Fig. 1; Table 1). They have a low content of primary matrix,

Table 1: List of the studied sandstone samples and their locations.

Sample	Sample locality	GPS coordinates
19-VD	Loc. *MK-12*; southern slope of the Klokoč hill; 425 m above sea level	N 48°28'401", E 17°19'181"
22-VD	Loc. *MK-15*; Sološnická dolina valley, right side of the Sklenný vrch hill; 457 m above sea level	N 48°27'008", E 17°17'556"
23-VD	Detto loc. *MK-15*	N 48°27'008", E 17°17'556"
31-VD	Loc. *MK-20*; left tributary of the Sološnická dolina valley, east of the Peterklin hill; 280 m above sea level	N 48°26'643", E 17°14'904"
32-VD	Loc. *MK-21*; southwestern ridge of the Klokoč hill, west of the Mesačná hill; 470 m above sea level	N 48°27'602", E 17°17'838"
33-VD	Loc. *MK-22*; south-west valley from the Klokoč hill; 444 m above sea level	N 48°27'422", E 17°17'942"

Table 2: Modal compositions of the studied Permian sandstones from the Malužiná Formation.

Sample	Qm (%)	Qp (%)	P (%)	K (%)	Lm (%)	Lv (%)	Mt (%)	Mc (%)
19-VD	56.0	17.0	10.1	13.9	0.0	0.0	2.0	1.0
22-VD	20.1	26.8	10.1	11.0	18.3	10.3	0.9	2.5
23-VD	26.1	21.0	10.8	12.1	13.0	8.3	0.4	8.3
31-VD	26.9	17.1	15.5	12.7	5.0	19.0	1.8	2.0
32-VD	37.9	26.7	10.4	17.4	1.7	3.9	1.4	0.6
33-VD	60.4	12.2	3.2	19.3	2.4	0.2	2.2	0.0

Explanations: Qm — monocrystalline quartz grains, Qp — polycrystalline quartz grains, P — plagioclase feldspar grains, K — potassium feldspar grains, Lm — metamorphic lithic grains, Lv — volcanic-hypabyssal lithic grains, Mt — matrix, Mc — mica. Abbreviations of petrofacies parameters (Q*p*, Q*m*, K, P) were used after Dickinson & Suczek (1979) and Dickinson (1985, 1988).

ranging from 0.4 to 2.2 % (Table 2). Quartz grains are the dominant detrital component, with monocrystalline (Q*m*) prevailing over polycrystalline (Q*p*) quartz. An exception is the sample 22-VD, where the Q*p* is dominant. The values of the Q*m*/Q*p* ratio vary in the range of 0.7–5.0. The fragments of potassium and Na-Ca feldspars are in equal abundances, but with potassium feldspars slightly prevailing over plagioclases. For this reason, the ratio of potassium feldspars (K) to plagioclases (P) shows mostly the values near 1 (K/P = 0.8–1.7).

However, in the sample 33-VD this ratio is higher than 5, as the potassium feldspar highly prevails (Table 2). The potassium feldspars in the studied samples are represented by orthoclase ($Ab_{10.2-3.4}An_{0.3-0.1}Or_{89.5-96.5}$) and by microcline. The Na-Ca feldspars correspond to albite–oligoclase ($An_{0.3-25.4}$). Generally, they manifest a low content of orthoclase component ($Or_{0.1-1.5}$). Alterations of detrital feldspars during post-sedimentary processes were studied by Vďačný (2013), who found that the secondary albitization of feldspars did not reflect diagenetic changes, but modification processes in the primary source area.

Clastic mica content varied in the range of 0–8 % (Table 2). Lithic fragments varies similarly. Volcanic rock fragments (0 to 19 %) are represented by acid, as well as andesite-basalt rocks. Likewise, the content of metamorphic rock fragments is irregular (0–18 %), among them, the different phyllites and metaquartzites are most widespread. Fragments of the fine-grained paragneisses and mica schists are present only in minor amounts. According to the mineral composition, the studied sandstones belong to the arkoses, subarkoses, lithic subarkoses, and feldspathic litharenites (classification after McBride 1963).

The assemblage of heavy minerals includes: biotite (29.5 ± 32 %), magnetite, ilmenite and hematite (27 ± 26 %), titanite (14 ± 12 %), tourmaline (10 ± 10 %), garnet (9 ± 8 %), apatite (6 ± 7 %), zircon (4 ± 3 %), and rutile (0.5 ± 0.9 %). These data represent the average from the ten analysed sandstone samples (Vďačný 2013).

Analytical technique

Monazite grains were only sporadically recorded in the heavy-mineral fraction using the gravity separation method in heavy liquids. The dried samples were sieved (0.063–0.250 mm) for the heavy mineral analyses. As the monazite formed the small grains (predominant 10–50 μm, seldom around 100 μm) and the relatively scarce larger grains were often destroyed during disintegration of the sandstones, monazites were not detected within the heavy mineral assemblage. Consequently, all analyses of monazites were carried out on the grains found in the polished thin sections by microprobe analysis.

Analyses of monazites were obtained using the electron microprobe Cameca SX-100 housed at the Department of Special Laboratories at the State Geological Institute of Dionýz Štúr (Geological Survey of Slovak Republic) in Bratislava. Monazite analyses suitable for dating have to meet some special analytical conditions. The counting time for Pb was extended to 300 s and the beam current adjusted to 180 nA. Accelerating voltage of 15 kV can efficiently excite the PbMa line. The beam diameter of 3 μm was used. These conditions form a compromise between two cases: maximizing counts while minimizing damage effect at the beam spot. The other elements involved in the dating calculations also had prolonged counting times, Th 35 s, U 90 s, Y 45 s. The following calibration standards (natural grains or synthetic compounds) and analytical lines were used: apatite (P$K\alpha$), wollastonite (Si$K\alpha$, Ca$K\alpha$), GaAs (As$L\alpha$), barite (S$K\alpha$, Ba$L\alpha$), Al_2O_3 (Al$K\alpha$), ThO_2 (Th$M\alpha$), UO_2 (U$M\beta$), cerusite (Pb$M\alpha$), YPO_4 (Y$L\alpha$), $LaPO_4$ (La$L\alpha$), $CePO_4$ (Ce$L\alpha$), $PrPO_4$ (Pr$L\beta$), $NdPO_4$ (Nd$L\alpha$), $SmPO_4$ (Sm$L\alpha$), $EuPO_4$ (Eu$L\beta$), $GdPO_4$ (Gd$L\alpha$), $TbPO_4$ (Tb$L\alpha$), $DyPO_4$ (Dy$L\beta$), $HoPO_4$ (Ho$L\beta$), $ErPO_4$ (Er$L\beta$), $TmPO_4$ (Tm$L\alpha$), $YbPO_4$ (Yb$L\alpha$), $LuPO_4$ (Lu$L\beta$), fayalite (Fe$K\alpha$) and $SrTiO_3$ (Sr$L\alpha$). Mutual interferences U-$M\beta$ with Th$M\alpha$, Th*M3-N4*, Th*M5-P3* and Pb$M\alpha$ with Th$M\zeta_1$, Th$M\zeta_2$, Y$L\gamma_{2,3}$ and various interferences between REE's were resolved by using correction coefficients derived by measurement on the calibration standards.

A complete analysis of monazite involving almost all elements present in monazite is obtained at each measurement spot. The age calculated from one point is referred to as the

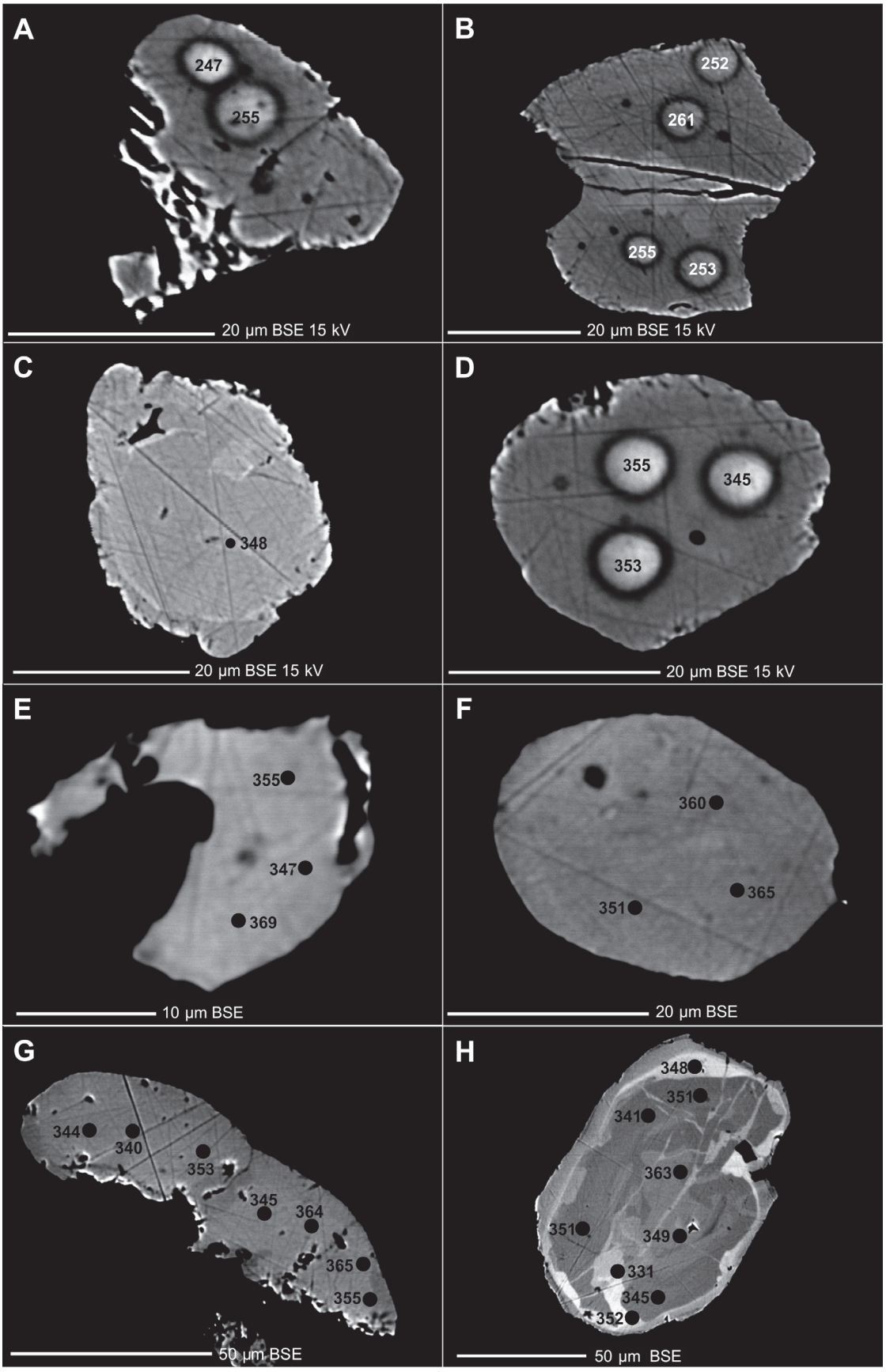

Fig. 2. BSE images showing the Permian (**A, B**) and the Variscan (**C–H**) monazites in various samples.

apparent age. Groups of the apparent ages plotted in a histogram indicate a single age population. An isochrone diagram provides a further test to distinguish single age populations. Points should plot on a single line crossing the zero coordinate. The method of age calculation based on the statistical approach was described by Montel et al. (1996). The precision of monazite dating was proven by dating of seven monazite standards dated by SHRIMP. The error in age was determined by error propagation from 2 σ errors obtained for measured Pb, Th and U though equation of age. For these elements the 2 σ error was added or subtracted, giving six concentrations that were used for the age determination in all possible mutual combinations. Finally, the age error was taken according to biggest deviation from the age obtained from measured Pb, Th and U concentrations.

Histograms and isochrones were constructed using the author's own unpublished software (Mondat in Excel spreadsheet, P. Konečný). Monazite age was calculated following the statistical procedure after Montel et al. (1996).

Monazite features and chemical composition

Dating of monazites from the MF sandstones revealed two distinct age populations, Permian and Carboniferous. The monazite populations differ in shape, zoning and chemical composition. The Carboniferous monazites are usually bigger, having the diameter from 20 to 120 μm and often showing a complex chemical zoning (BSE images, Fig. 2H). On the other hand, monazites of Permian age are smaller, with a size of about 10 to 30 μm, and have homogeneous composition. Only few grains show zoning in BSE images. Although the monazites of the both age populations are chemically similar, they have some specific features. The range of Th* presented in the isochrone diagrams (Figs. 4, 5) is very wide for the Carboniferous monazites from 3.98 to 11.27 Th*, whereas the Permian monazites have lower Th* limited to a range from 2.85 to 6.07 and one grain with 8.58. ThO_2 content is similar in both monazite groups. For the Carboniferous monazites the average ThO_2 is 4.8 wt. % (min 2.1, max 10.2) and for Permian average content is 4.6 wt. % (min 2.5, max 6.5). The Carboniferous monazites are roughly three times more enriched in UO_2, with the average for the Carboniferous monazites 0.66 wt. % (min 0.16, max 2.43) and for the Permian monazites 0.26 wt. %.

The Carboniferous monazites contain slightly less REE's than the Permian ones. Enrichment in REE for the Permian monazites is due to higher content of La and Ce. Average content of La_2O_3 for the Carboniferous monazites is 13.23 wt. % (min 11.04, max 15.99) and for the Permian 14.49 wt. % (min 11.04, max 17.80). Ce behaves similarly, the Carboniferous monazites have an average Ce_2O_3 of 28.24 wt. % (min 25.79, max 30.17), the average for the Permian grains is 29.59 wt. % Ce_2O_3 (min 26.46, max 32.69). Abundance of Pr, Nd and Sm is almost identical for the both age groups. Yttrium is higher in the Carboniferous monazites with average of 1.61 wt. % Y_2O_3 (min 0.42, max 2.96) and 1.36 wt. % (min 0.18, max 3.87) for the Permian monazites. The monazites of Carboniferous and Permian age contain negligible concentrations of S and Sr. Some of the monazites have As up to 0.1 wt. %.

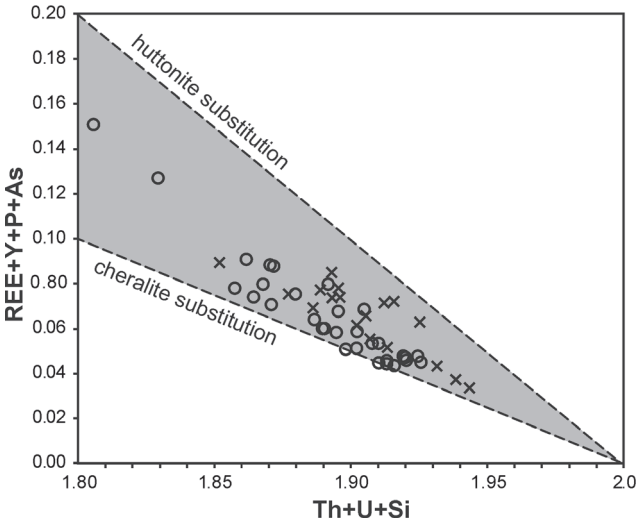

Fig. 3. Substitutions in monazites from the Malužiná Formation sandstones. Different symbols refer to the Mississippian (*cross*) and Permian monazites (*circle*).

Monazite compositional variations are affected by the substitution processes. The most common substitutions are huttonite and cheralite substitutions (after Linthout 2007). The composition of the Carboniferous and the Permian monazites involves both types of substitutions (Fig. 3). The Carboniferous monazites tend to follow the huttonite exchange vector, while the Permian monazites are shifted towards the cheralite substitution.

Monazite dating

Monazite dating presented on a histogram proves two main events: Carboniferous and Permian.

A substantial part of the analysed monazites (54 out of 72 data, that is about 70 % of all measurements) showed the peak of Variscan age, in the histogram with dominance of apparent ages in the range of 340–371 Ma (Fig. 4, Table 3 — *only as a Suplemment in the electronical version; www.geologicacarpathica.com*), which corresponds to the interval from Famennian to Lower Visean according to the International Stratigraphic Chart (2008). Some outliers occur on both sides of the age histogram. Two monazite ages were somewhat older, 391 Ma (sample 33-VD) and 401 Ma (sample 31-VD) which correspond to the boundary of the Lower/Middle Devonian (Emsian–Givetian).

Likewise, no more than four grains showed younger ages, spanning the range from 311 to 323 Ma, that corresponds to the Serpukhovian–Bashkirian according to the International Stratigraphic Chart (2008). The Variscan age calculated for monazites within the interval 330–380 Ma from 48 grains (Fig. 4) is 351 ± 3.3 Ma, corresponds to the earliest Tournaisian, or the stratigraphic boundary between the Devonian and the Carboniferous (Famennian–Tournaisian). The wide range of Th* enables us to construct an isochron which crosses the origin at a very small deviation +33 ppm Pb (equation of the linear trend is $y = 0.0151x + 0.0033$).

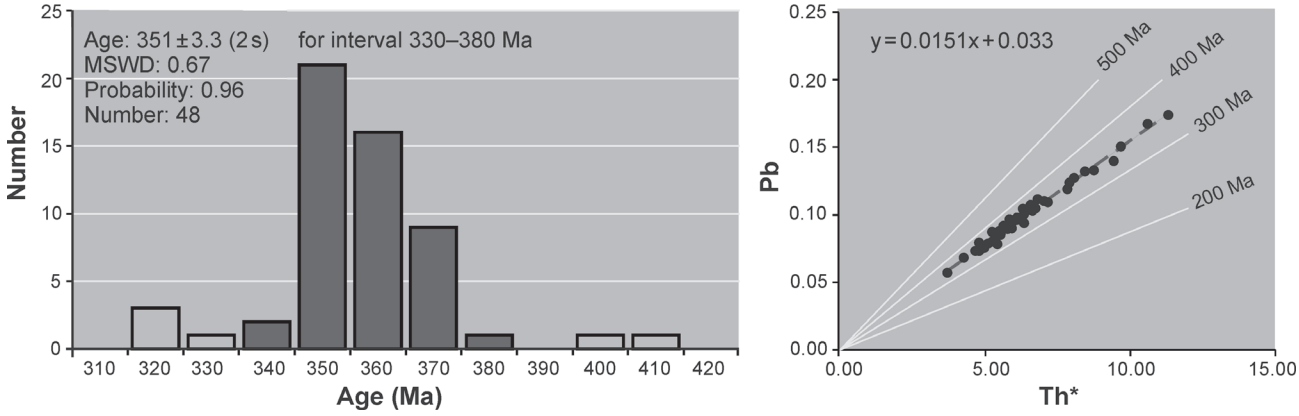

Fig. 4. A — Histogram showing the whole distribution of the Variscan EMPA monazite ages obtained from the Malužiná Formation sandstones, with indication of the peak ages (data source see Table 3). **B** — Pb *vs* Th* plot of single analyses and drawn isochrones from 100 to 500 Ma. Th* is given by measured Th plus added U recalculated to Th equivalent concentration, after natural decay leading to Pb production.

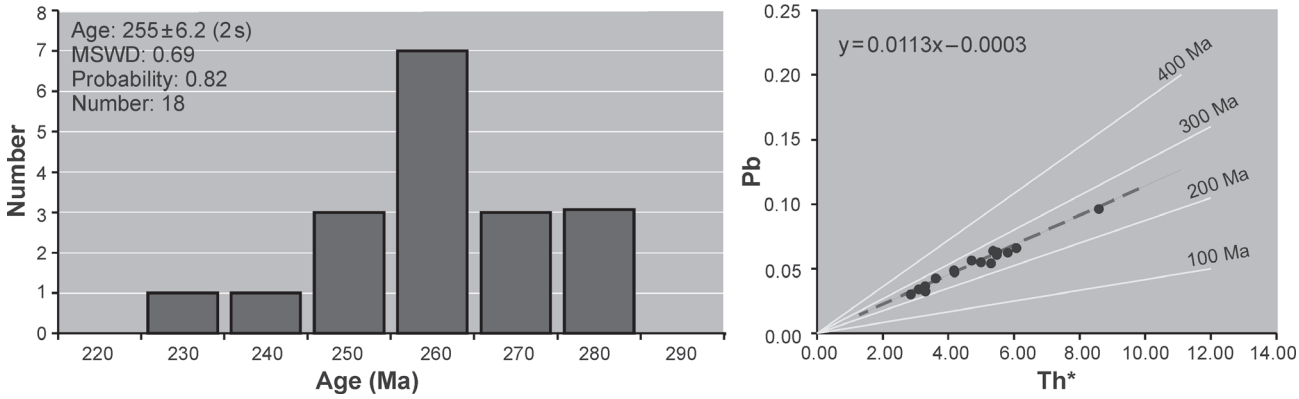

Fig. 5. A — Frequency diagrams of the Permian/Triassic monazite ages in the Malužiná Formation sandstone samples (data source see Table 3). **B** — Pb *vs* Th* plot of single analyses and drawn isochrones from 100 to 500 Ma. Th* is given by measured Th plus added U recalculated to Th equivalent concentration, after natural decay leading to Pb production.

Besides the Devonian-Carboniferous ages, Permian ages (Table 3) were also detected in the two samples (19-VD and 22-VD). Histogram (Fig. 5) presents the significant maximum around 255 Ma. The weighted average corresponds to 255±6.2 Ma. All data represent a perfect, almost ideal isochron with parameters y=0.0113x+0.0003 which crosses the origin at +3 ppm Pb.

Only a few measurements gave the Triassic ages in the interval 240–230 Ma. Because the samples containing monazite with Triassic ages are situated either directly along the thrust nappe plane of the Hronicum Unit (22-VD) or within the zone of Cu±U-bearing mineralization (19-VD), we suppose that these ages reflect the local alterations of the Permian detrital monazite by the circulations of the low-temperature hydrothermal fluids.

Discussion

***Variscan provenance*:** Age data as inferred from the chemical monazite dating of the Permian clastic sediments of the Hronicum Unit are practically missing. Only Olšavský (2008) in his Ph.D. Thesis (results previously presented at the 6th Anniversary seminary of the Slovak Geological Society — Demko & Olšavský 2007) provided about 40 monazite ages from the southern slopes of the Nízke Tatry Mts, but only in the form of a enclosed histogram and without an accompanying table of complete data on chemical composition. Also with respect to interpretation, it is important to state here that these monazite ages came from rhyolite fragments separated from gravel material in the MF coarse-grained conglomerates, from the hanging wall of andesite/basalts of the second eruption phase at the locality of Bystrá-Stupka. Olšavský's (2008) data show the bimodal dispersal of monazite ages. The first group hints at the Permian ages, with a striking peak at 290 Ma, in the range of 230–290 Ma, with the weighted average of 257±9 Ma (20 analyses). The second age group displays the peak at 360 and 340 Ma, whereby age dispersal is relatively wide (from 310 to 370 Ma), with the weighted average of 342±12 Ma (22 analyses), corresponding to the Visean. Detected age maxima suggest two phases of volcanic activity: one phase took place in the Cisuralian and the second one in the Mississippian.

Basically, very similar age data were also detected from detrital monazites of the MF sandstones in the Malé Karpaty

Mts. The weighted average monazite age of 351 ± 3.3 Ma (Fig. 4), detected in the sandstone samples of the MF in the Malé Karpaty Mts, is similar to the monazite ages inferred from the rhyolite pebbles of the MF on the southern slopes of the Nízke Tatry Mts. It is unquestionable that the detected Mississippian monazite ages indicate the age of the source area of the MF sediments. It is evident that acid volcanic rocks are one of the sources, as described in the case of occurrences of the MF on the southern slopes of the Nízke Tatry Mts by Olšavský (2008). In the studied MF sandstones from the Malé Karpaty Mts, content of acid volcanic fragments vary in the range from 0 to 19 volumetric % (Table 2). However, it is important to stress that fragments of rhyolites represent a common component of the clastic detritus in the whole profile of the MF Permian sediments of the Hronic Unit, not only in the form of pebbles in conglomerates but also in the form of lithic grains in sandstones (Ďurovič 1971; Vozárová & Vozár 1988; Vozárová 1990, 1998; Olšavský 2008; Vďačný 2013; Vďačný et al. 2013).

In the pre-Pennsylvanian crystalline basement of the central Western Carpathians, several low-grade metamorphosed complexes occur (confr. Biely et al. 1996), that mostly emerge in the form of tectonically restricted slices on the middle- and higher metamorphosed complexes, or they lie directly on granitoids. Some of them even show features of contact metamorphosis. In fact, products of acid volcanism were found only in the Jánov Grúň Complex (Bajaník et al. 1979; Miko 1981) in the Kráľovohoľské Tatry Mts and in the Krakľová Formation (Korikovskij & Miko 1992), both emerging in the Northern Veporic Unit. The volcanics together with their effusive members make up conformal layers with metasediments, alternating with each other, as is usual with synsedimentary volcanism. On the basis of pollen analysis of associated metasediments, the Jánov Grúň Complex was broadly stratigraphically classified into the Upper Silurian to the Mississippian (Klinec et al. 1975; Planderová & Miko 1977). Likewise, on the basis of the U-Pb (SHRIMP) zircon ages, the Mississippian age of 358.7 ± 3.9 Ma was detected from the metarhyolites of the low-grade crystalline basement of the Krakľová Zone from the Volchovo valley (Vozárová et al. 2010). Biostratigraphically well documented Mississippian metasediments are known only from the Northern Gemeric Unit (Bouček & Přibyl 1960; Kozur et al. 1976; Bajaník & Planderová 1985; Mamet & Mišík 2003). They were originally described as the Ochtiná Formation (Bajaník et al. 1981) and later were redefined as the separate Ochtiná Group (Vozárová 1996). However, the problem remains that no synsedimentary acid volcanics are known within the Ochtiná Group sequence.

Monazite ages from the rhyolite fragments detected on the southern slopes of the Nízke Tatry Mts (Demko & Olšavský 2007; Olšavský 2008) and also from sandstones of the MF in the Malé Karpaty Mts given in the present work, are in agreement with the upper boundary of the stratigraphic classification of microflora from the Jánov Grúň Complex. We assume that low-grade crystalline complexes must have existed in the source area of the MF sediments. They were similar to the occurrences in the Krakľová and Ľubietová Zones of the crystalline basement of the Northern Veporic Unit that included horizons with acid volcanism of the Mississippian age.

However, the acid volcanites were not the exclusive source of detrital monazite. In comparison with rhyo-dacitic detritus, detrital material derived from granitoid complexes (potassium feldspars, Na-Ca feldspars, clastic mica), is the substantially more conspicuous clastic component in the sandstones of the MF (Table 2). Likewise, granitoid pebbles are common in associated conglomerates. No doubt a substantial part of the detrital monazites were derived from the plutonic complexes.

In the Western Carpathians, magmatic plutons intruded into the high- to medium-grade crystalline basement made of upper- and middle-crustal Variscan nappes (Bezák et al. 1997) which show distinct southern vergency (Siegl 1982; Putiš 1992; Bezák et al. 1997; Bielik et al. 2004). The prevailing granitoids are petrochemically classified as the S-types. Granodiorite-tonalite I-types are relatively less represented. Permian A-type granitoides and volcanics are spatially least wide-spread (Broska & Uher 2001; Poller et al. 2002; Kohút & Stein 2005; Radvanec et al. 2009; Uher et al. 2009; Vozárová et al. 2009, 2012). U-Pb zircon radiometric datings confirmed the range from Devonian to Permian for the Variscan magmatic period in the Western Carpathians (Bibikova et al. 1988; Kohút et al. 1997, 2009; Kráľ et al. 1997; Poller & Todt 2000; Gaab et al. 2006; Broska et al. 2013 and references therein). According to the original age data, it was assumed that S-type granitoids are systematically older, with the range of 340–367 Ma, while I-types of granitoids are younger, with the range of 303–345 Ma. Likewise, monazite ages also showed similar age discrepancies, with the range of 333–367 Ma for S-types and of 308–345 Ma for I-types (Finger et al. 2003 and references therein). However, this assumption of different ages for S- and I-types of granitoids was rebutted by new SIMS U-Pb zircon ages that confirmed the Mississippian age, within the range of 367–353 Ma also for I-type granitoids. Therefore, almost the same age was documented for both I- and S-type magmatites (Broska et al. 2013).

The ages of detrital monazites detected in the MF sandstones from the Malé Karpaty Mts dominantly span the range from 340 to 370 Ma. This is the period that covers the maximal intensity of the Variscan polyphase magmatic activity in the Western Carpathians. Petrofacies analyses of the Permian sandstones from the Hronicum Unit in all occurrences in the Western Carpathians suggest provenances either from dissected magmatic arc or active continental margin (Vozárová & Vozár 1988; Vozárová 1990; Vďačný et al. 2013). Mixing of magmatogenic and volcanogenic detritus, associated only with a small amount of low- to medium-grade metamorphic clasts is characteristic (Dickinson & Suczek 1979; Dickinson 1985, 1988; Ingersoll 1990). The chemical composition of clastic detritus in the MF sandstones from the Malé Karpaty Mts also indicates the acid to intermediate magmatic provenance, similar to active continental margin (Vďačný et al. 2013). On the basis of petrochemical data and age of detrital monazites, we can infer the source area of the MF sandstones to be most likely derived from I-type magmatism associated with the Variscan subduction processes and with the origin of magmatic arc in the Mississippian. Stampfli (2012) regards I-types granitoids as

an indicator of the onset of the subduction process of the Prototethys. Alternatively, Broska et al. (2013) also infer formation of I-type granitoids in the Western Carpathians from the Variscan magmatic arc, as a result of collision of the Prototatricum crust (the term Prototatricum was used by these authors for the common Variscan basement of the Tatric and the Veporic Units) which was a part of the Galatian superterrane, with the oceanic crust of the Prototethys.

The metarhyodacite fragments occur, as a whole, in the Pennsylvanian-Permian clastic sediments of the Hronicum Unit in the Western Carpathians and it is considered that acid volcanism was synchronous with the main magmatic events in the Mississippian. These volcanic centers were probably situated in the former back-arc basins on the continental crust or directly in the intra-arc environment. In the Veporicum Unit the low-grade acid volcanite-bearing crystalline complexes were tectonically overthrusted onto the higher-grade crystalline complexes. This was a result of not only Alpine but also probably already Variscan tectonics as a part of them were overlapped by the Permian sediments.

***Permian provenance*:** The Permian monazite ages show the significant maximum at 255 Ma, with the weighted average of 255 ± 6.2 Ma. Monazites were most likely derived from synsedimentary volcanic sources that could be situated on the margins of the original Pennsylvanian-Permian sedimentary rift of the Hronicum Unit. These monazite age data are similar to the 260 Ma of $^{87}Rb/^{86}Sr$ age of the basalt sample from the 2nd eruption phase (Vozárová et al. 2007) and roughly correspond to radiometric U-Pb dating of the uranium mineralization (Legierski in Rojkovič 1997 — Kravany Beds, 263–274 Ma) from the Nízke Tatry Mts.

The original sedimentary basin of the Ipoltica Group, based on the characteristic sedimentary filling, as well as the distribution of sedimentary lithofacies and narrow connection with linear continental tholeiitic volcanism, permits to incorporate this sedimentary basin into the regional rift system of several kilometers long. Marginal parts and basement of the original sedimentary basin were tectonically cut off due to the Alpine nappe stacking. In the recent structure of the Western Carpathians, the rootless nappes of the Hronicum Unit (Biely & Fusán 1967; Biely et al. 1968; Andrusov et al. 1973) have preserved only the central parts of the original sedimentary basin, with its occurrences of andesite-basalt continental tholeiites. The acid volcanites, belonging to the supposed primary bimodal volcanic association, are only present as the redeposited rhyo-dacite detritus in clastic sediments (pebbles, sand grains).

A small number of monazite grains show analytical spots with younger ages (Fig. 2A), within the interval of 230–240 Ma. This rejuvenation reflects an alteration of the original Permian monazites by the circulated low-thermal fluids during diagenetic processes. These younger monazite ages were mainly detected on the grains from the area of synsedimentary Cu ± U mineralization (west and southwest from Sološnica; Rojkovič 1997 and references therein). Because the Hronicum Permian sedimentary basin was situated in arid climatic conditions as a whole, the circulated diagenetic fluids were characterized by high salinity. Thus, the highly saline brines could have started the rejuvenation of the Permian detrital monazite by migration of some elements. A detailed explanation of this process was described by Mathieu et al. (2001) in U deposits of the Franceville basin, Gabon.

Conclusions

The chemical ages of detrital monazites from the MF Permian sandstones of the Hronic Unit in the Malé Karpaty Mts show two maxima: i) Variscan ages with maximal peaks in the range of 370–340 Ma, with a weighted average of 351 ± 3.3 Ma and, ii) Permian ages in the interval of 280–250 Ma, with the distinct peak at 255 Ma. These two age groups reflect several different sources of clastic detritus for the Permian sediments of the Hronicum Unit. Variscan magmatic rocks, bounded with subduction-collisional magmatic arc, appear to be the main source. They correspond to zircon and also monazite ages described from I-type magmatites of the Western Carpathians. Presumably, the partial mixture with an S-type magmatic source cannot be excluded. The same Variscan monazite age was derived from the acid metavolcanic rocks connected with the low-grade metamorphic crystalline complexes. The additional sources were the Permian rhyo-dacite synsedimentary volcanic centers, situated on the rifted, fault-bordered margins of the original sedimentary basin.

The Permian rift-related sedimentary basin of the Hronicum Unit was situated in a foreland retro-arc setting on the Prototatricum (in the sense of Broska et al. 2013) continental crust. This sedimentary basin was filled with clastic detritus derived from a dissected Mississippian magmatic arc and Permian synsedimentary volcanic centers.

Acknowledgments: We would like to express our gratitude to the reviewers F. Finger, R. Čopjaková and I. Broska for their helpful and critical comments on the earlier versions of the manuscript. This work was supported by the Slovak Research and Development Agency under the Contract No. APVV-0546-11 and the Slovak Scientific Grant Agency (Grant No. VEGA-1/0095/12).

References

Andrusov D., Bystrický J. & Fusán O. 1973: Outline of the structure of the West Carpathians. In: Guidebook for Geological Excursion, X. Congress of CBGA. *D. Štúr Inst. Geol.,* Bratislava, 1–44.

Bajaník Š. & Planderová E. 1985: Stratigraphic position of the lower part of the Ochtiná Formation (between Magnezitovce and Magura). *Geol. Práce, Spr.* 82, *GÚDŠ*, Bratislava, 67–76 (in Slovak).

Bajaník Š., Vozárová A. & Reichwalder P. 1981: Lithostratigraphic classification of the Rakovec Group and Late Paleozoic sediments in the Spišsko-gemerské rudohorie Mts. *Geol. Práce, Spr.* 75, 27–56 (in Slovak).

Bajaník Š., Biely A., Miko O. & Planderová E. 1979: About Paleozoic volcanic-sedimentary Predná Hola Complex (Nízke Tatry Mts.). *Geol. Práce, Spr.* 73, 7–28 (in Slovak).

Bezák V., Jacko S., Janák M., Ledru P., Petrík I. & Vozárová A. 1997: Main Hercynian lithotectonic units of the Western Car-

pathians. In: Grecula P., Hovorka D. & Putiš M. (Eds.): Geological evolution of the Western Carpathians. *Miner. Slovaca, Monograph,* Bratislava, 261–268.

Bibikova E.V., Cambel B., Korikovsky S.P., Broska I., Gracheva T.V., Makarov V.A. & Arakeliants M.M. 1988: U-Pb and K-Ar isotopic dating of Sinec (Rimavica granites) (Kohút zone of Veporides). *Geol. Zbor. Geol. Carpath.* 39, 147–157.

Bielik M., Šefara J., Kováč M., Bezák V. & Plašienka D. 2004: The Western Carpathians — interaction of Hercynian and Alpine processes. *Tectonophysics* 393, 63–86.

Biely A. & Fusán O. 1967: Zum Problem der Wurzelzonen der subtatrischen Decken. *Geol. Práce, Spr.* 42, 51–64.

Biely A., Bystrický J. & Fusán O. 1968: Zur Problematik der "subtatrischen Decken" in den Westkarpaten. *Geol. Zbor. Geol. Carpath.* 19, 295–296.

Biely A., Bezák V., Elečko M., Gross P., Kaličiak M., Konečný V., Lexa J., Mello J., Nemčok J., Potfaj M., Rakús M., Vass D., Vozár J. & Vozárová A. 1996: Explanations to Geological Map of Slovakia, 1:500,000. In: Biely A. (Ed.): Ministry of Environment of Slovak Republic — Geological Survey of Slovak Republic. *Dionýz Štúr Publ.*, Bratislava, 1–76.

Bouček B. & Přibyl A. 1960: Revision der Trilobiten aus dem slowakischen Oberkarbon. *Geol. Práce, Spr.* 20, 5–50.

Broska I. & Uher P. 2001: Whole-rock chemistry and genetic typology of the West-Carpathian Variscan granites. *Geol. Carpathica* 52, 79–90.

Broska I., Petrík I., Beeri-Shlevin Y., Majka J. & Bezák V. 2013: Devonian/Mississippian I-type granitoides in the Western Carpathians: A subduction-related hybrid magmatism. *Lithos* 162–163, 27–36.

Demko R. & Olšavský M. 2007: The question of rhyolite detritus in the Malužiná Formation. *Miner. Slovaca* 39, 4, *Geovestník,* 8–9 (in Slovak).

Dickinson W.R. 1985: Interpreting provenance relations from detrital modes of sandstones. In: Zuffa G.G. (Ed.): Provenance of Arenites. *Reidel,* Dordrecht, 333–361.

Dickinson W.R. 1988: Provenance and sediment dispersal in relation to paleotectonics and paleogeography of sedimentary basins. In: Kleinspehn K.L. & Paola C. (Eds.): New perspectives in basin analysis. *Springer-Verlag*, New York, 3–25.

Dickinson W.R. & Suczek C.A. 1979: Plate tectonics and sandstone compositions. *Amer. Assoc. Petrol. Geol. Bull.* 63, 2164–2182.

Dostal J., Vozár J., Keppie J.D. & Hovorka D. 2003: Permian volcanism in the Central Western Carpathians (Slovakia): Basin-and-Range type rifting in the southern Laurussian margin. *Int. J. Earth Sci. (Geol. Rundsch.)* 92, 27–35.

Ďurovič V. 1971: Sedimentary-petrographic research of the volcano-sedimentary (melaphyre) series in the central Western Carpathians. *Acta Geol. Geogr. Univ. Comen. Bratislava* 23, 5–114 (in Slovak).

Finger F., Broska I., Haunschmid B., Hraško Ľ., Kohút M., Krenn E., Petrík I., Riegler G. & Uher P. 2003: Electron-microprobe dating of monazites from Western Carpathians basement granitoids: plutonic evidence for an important Permian rifting event subsequent to Variscan crustal anatexis. *Int. J. Earth Sci. (Geol. Rundsch.)* 92, 86–98.

Gaab A.S., Poller U., Janák M., Kohút M. & Todt W. 2006: Zircon U-Pb geochronology and isotopic characterization for the pre-Mesozoic basement of the Northern Veporic Unit (Central Western Carpathians, Slovakia). *Schweitz. Mineral. Petrogr. Mitt.* 85, 69–88.

Ingersoll R.V. 1990: Actualistic sandstone petrofacies: discriminating modern and ancient source rocks. *Geology* 18, 733–736.

Klinec A., Planderová E. & Miko O. 1975: Lower Paleozoic age of the Hron Complex in the veporides. *Geol. Práce, Spr.* 63, 95–104 (in Slovak).

Kohút M. & Stein H. 2005: Re-Os molybdenite dating of granite-related Sn-W-Mo mineralisation at Hnilec, Gemeric Superunit, Slovakia. *Miner. Petrology* 85, 117–129.

Kohút M., Kovach V.P., Kotov A.B., Salnikova E.B. & Savatenkov V.M. 1997: Sr and Nd isotope geochemistry of Variscan granitic rocks from the Western Carpathians — implications for granite genesis and crustal evolution. *Geol. Carpathica* 50, 477–487.

Kohút M., Uher P., Putiš M., Ondrejka M., Sergeev S., Larionov A. & Paderin I. 2009: SHRIMP U-Th-Pb zircon dating of the granitoid massifs in the Malé Karpaty Mountains (Western Carpathians): evidence of Meso-Hercynian successive S- to I-type granitic magmatism. *Geol. Carpathica* 60, 345–350.

Korikovskij S.P. & Miko O. 1992: Low-grade metasediments of the Kraklová Formation of Veporic crystalline complex. *Miner. Slovaca* 24, 381–391 (in Slovak).

Kozur H., Mock R. & Mostler H. 1976: Stratigraphische Neueinstufung der Karbonatgesteine der unteren Schichtenfolge von Ochtiná (Slowakei) in das oberste Vise-Serpukhovian (Namur A). *Geol. Paläont. Mitt. Innsbruck* 6, 1–29.

Kráľ J., Hess C., Kober B. & Lippolt H.J. 1997: $^{207}Pb/^{206}Pb$ and $^{40}Ar/^{39}Ar$ age data from plutonic rocks of the Strážovské vrchy Mts. basement, Western Carpathians. In: Grecula P., Hovorka D. & Putiš M. (Eds.): Geological evolution of the Western Carpathians. *Miner. Slovaca, Monograph,* Bratislava, 253–260.

Krenn E., Ustaszewski K. & Finger F. 2008: Detrital and newly formed metamorphic monazite in amphibolite facies metapelites from the Motajica Massif, Bosnia. *Chem. Geol.* 254, 164–174.

Linthout K. 2007: Tripartite division of the system of the 2REE-PO_4–$CaTh(PO_4)_2$–$2ThSiO_4$, discreditation of brabantite and recognition of cheralite as the name for members dominated by $CaTh(PO_4)_2$. *Canad. Mineralogist* 45, 503–508.

Mamet B. & Mišík M. 2003: Marine Carboniferous algae from metacarbonates of the Ochtiná Formation (Gemeric Unit, Western Carpathians). *Geol. Carpathica* 54, 3–8.

Mathieu R., Zellerström L., Cuney M., Gauthier-Lafaye F. & Hidaka H. 2001: Alteration of monazite and zircon and lead migration as geochemical tracers of fluid paleocirculations around the Oklo-Okélombo and Bangombénatural nuclear reaction zones (Franceville basin, Gabon). *Chem. Geol.* 171, 147–171.

McBride E.F. 1963: A classification of common sandstones. *J. Sed. Petrology* 33, 664–669.

Miko O. 1981: Middle Paleozoic volcanic-sedimentary Jánov Grúň Formation in the Veporic crystalline of the Nízke Tatry Mts. [Srednepaleozojskaja vulkanogenno-osadočnaja tolšča Janovogo Grunja v veporidnom kristalinike Nízkych Tatr.] *Geol. Zbor. Geol. Carpath.* 32, 465–474 (in Russian).

Montel J.M., Foret S., Veschambre M., Nicollet Ch. & Provost A. 1996: Electron microprobe dating of monazite. *Chem. Geol.* 131, 37–53.

Morton A.C. & Hallsworth C.R. 1999: Processes controlling the composition of heavy mineral assemblages in sandstones. *Sed. Geol.* 124, 3–29.

Olšavský M. 2008: Facial analysis of depositional sequences of the Malužiná Formation and their geological setting at northeastern slopes of the Nízke Tatry Mts. *Unpubl. Diz. Thesis. Comenius University in Bratislava, Faculty of Natural Sciences*, 1–194 (in Slovak).

Planderová E. & Miko O. 1977: New information on the age of the Veporic crystalline rocks based on pollen analysis. *Miner. Slovaca* 9, 275–292 (in Slovak).

Poller U. & Todt W. 2000: U-Pb single zircon data of granitoids from the High Tatra Mountains (Slovakia): implications for the geodynamic evolution. *Trans. Earth Sci. Roy. Soc. Edinburgh* 91, 235–243.

Poller U., Uher P., Broska I., Plašienka D. & Janák M. 2002: First Permian-Early Triassic ages for tin-bearing granites from the

Gemeric unit (Western Carpathians, Slovakia): connection to the post-collisional extension of the Variscan orogeny and S-type granite magmatism. *Terra Nova* 14, 410–418.

Prokešová R., Plašienka D. & Milovský R. 2012: Structural pattern and emplacement mechanism of the Krížna cover nappe (Central Western Carpathians). *Geol. Carpathica* 63, 1, 13–32.

Putiš M. 1992: Variscan and Alpidic nappe structures of the Western Carpathians crystalline basement. *Geol. Carpathica* 43, 369–380.

Radvanec M., Konečný P., Ondrejka M., Putiš M., Uher P. & Németh Z. 2009: The Gemeric granites as an indicator of the crustal extension above the Late Variscan subduction zone and during the Early Alpine riftogenesis (Western Carpathians): An interpretation from the monazite and zircon ages dated by CHIME and SHRIMP methods. *Miner. Slovaca* 41, 381–394 (in Slovak).

Rasmussen B. & Muhling J.R. 2009: Reactions destroying detrital monazite in greenschist-facies sandstones from the Witwatersrand basin, South Africa. *Chem. Geol.* 264, 311–327.

Rojkovič I. 1997: Uranium mineralization in Slovakia. *Acta Geol. Univers. Comen., Monogr*., Bratislava, 1–117.

Rubato D., Williams I.S. & Buick I.S. 2001: Zircon and monazite response to prograde metamorphism in the Reynolds Range, Central Australia. *Contr. Mineral. Petrology* 140, 458–468.

Siegl K. 1982: Structure of the Vepor pluton (West Carpathians). *Geol. Zbor. Geol. Carpath.* 33, 171–175.

Stampfli G.M. 2012: The geodynamic of Pangea formation. *Géol. France* 1, 206–209.

Uher P., Ondrejka M. & Konečný P. 2009: Magmatic and post-magmatic Y-REE-Th phosphate, silicate and Nb-Ta-Y-REE oxide minerals in A-type metagranites: an example from the Turčok massif, the Western Carpthians, Slovakia. *Miner. Mag*., London 73, 6, 1009–1025.

Vďačný M. 2013: Provenance of the Malužiná Formation sandstones (Western Carpathians, Slovakia): constraints from standard petrography, cathodoluminescence imaging, and mineral chemistry of feldspars. *Geol. Quart.* 57, 61–72.

Vďačný M., Vozárová A. & Vozár J. 2013: Geochemistry of the Permian sandstones from the Malužiná Formation in the Malé Karpaty Mts (Hronic Unit, Western Carpathians, Slovakia): implications for source-area weathering, provenance and tectonic setting. *Geol. Carpathica* 64, 1, 23–38.

Vozár J. 1977: Tholeiitic magmatic rocks in the Permian of the Choč Nappe (Western Carpathians). *Miner. Slovaca* 9, 241–258 (in Slovak).

Vozár J. 1997: Rift-related volcanism in the Permian of the Western Carpathians. In: Grecula P., Hovorka D. & Putiš M. (Eds.): Geological evolution of the Western Carpathians. *Miner. Slovaca, Monograph*, 225–234.

Vozárová A. 1990: Significance of clastic petrofacies for the reconstruction of paleotectonic development of the Late Paleozoic of the Western Carpathians. In: Jablonský J. & Sýkora M. (Eds.): Sedimentary problems of the Western Carpathians. *D. Štúr Inst. Geol.*, Bratislava, 69–78 (in Slovak).

Vozárová A. 1996: Tectono-sedimentary evolution of Late Paleozoic basins based on interpretation of lithostratigraphic data (Western Carpathians, Slovakia). *Slovak Geol. Mag.* 3–4, *D. Štúr Publ*., Bratislava, 251–271.

Vozárová A. 1998: Late Carboniferous to Early Permian time interval in the Western Carpathians: Northern Tethys margin. In: Crasuin-Soleau S., Izart A., Vaslet D. & DeWever (Eds.): Peri-Tethys: stratigraphic correlations. 2. *Geodiversitas* 20, 4, 621–641.

Vozárová A. & Vozár J. 1981: Lithostratigraphical subdivision of the Late Paleozoic sequences of the Hronicum. *Miner. Slovaca* 13, 385–403 (in Slovak).

Vozárová A. & Vozár J. 1988: Late Paleozoic in West Carpathians. *D. Štúr Inst. Geol., Monograph,* Bratislava, 1–314.

Vozárová A., Kráľ J. & Vozár J. 2007: Sr isotopic composition in basalts of the Hronicum. *PETROS, Petrological Symposium, Abstracts Faculty of Natural Science, Geol. Inst., Slovak Acad. Sci.,* Bratislava, 22 (in Slovak).

Vozárová A., Šmelko M. & Paderin I. 2009: Permian single crystal U-Pb zircon age of the Rožňava Formation volcanites (Southern Gemeric Unit, Western Carpathians, Slovakia). *Geol. Carpathica* 60, 439–448.

Vozárová A., Lepekhina E., Vozár J. & Rodionov N. 2010: In situ U-Pb (SHRIMP) zircon age dating from the Permian volcanites of the Northern Veporicum. In: Kohút M. (Ed.): Dating 2010. Dating of minerals and rocks, metamorphic, magmatic and metallogenic processes, as well as tectonic events. *Conference Proceedings, State Geol. Inst. D. Štúr*, Bratislava, 49.

Vozárová A., Šmelko M., Paderin I. & Larionov A. 2012: Permian volcanics in the Northern Gemericum and Bôrka Nappe system: U-Pb zircon dating and implication to geodynamic evolution (Western Carpathians, Slovakia). *Geol. Carpathica* 63, 191–200.

Williams I.S. 2001: Response of detrital zircon and monazite, and their U-Pb isotopic systems, to regional metamorphism and host-rock partial melting, Cooma Complex, southeastern Australia. *Aust. J. Earth Sci.* 48, 557–580.

Wing B.A., Ferry J.M. & Harrison T.M. 2003: Prograde destruction and formation of monazite and allanite during contact and regional metamorphism of pelites: petrology and geochronology. *Contr. Mineral. Petrology* 145, 228–250.

Electronic supplement

VOZÁROVÁ et al.: Provenance of Permian Malužiná Formation sandstones (Hronicum, Western Carpathians): evidence from monazite geochronology

Appendix 1

Table 3: Microprobe analyses of monazites from the Malužiná Formation sandstones used for monazite dating. All analyses calculated on the 16 oxygen. **Abbreviations:** *bdl.* — denotes below detection limit. C. — Carboniferous; P. — Permian.

Sample	19-VD																								
Point	1/1 C.	2/1 C.	2/2 C.	3/1 C.	3/2 C.	4/1 P.	4/2 P.	5/1 C.	6/1 C.	7/1 P.	8/1 P.	9/1 C.	10/1 P.	11/1 P.	8/1 P.	9/1 C.	10/1 P.	4/3 P.	7/2 P.	8/2 P.	9/2 C..	10/2 P.	10/3 P.	11/2 P.	11/3 P.	11/4 P.
P_2O_5	30.02	29.21	29.12	29.02	29.21	28.61	28.61	28.20	28.35	30.22	30.19	29.50	29.43	29.90	30.19	29.50	29.43	29.02	29.81	29.64	29.30	29.41	29.36	29.29	29.45	28.93
As_2O_5	0.13	0.15	0.14	0.13	0.15	0.14	0.15	0.13	0.14	0.13	0.14	0.14	0.14	0.14	0.14	0.14	0.14	0.15	0.13	0.15	0.15	0.14	0.15	0.15	0.14	0.15
SiO_2	0.47	0.45	0.46	0.57	0.49	0.76	0.67	1.14	0.87	0.39	0.20	0.59	0.55	0.40	0.20	0.59	0.55	0.75	0.22	0.21	0.73	0.51	0.62	0.72	0.60	0.93
ThO_2	6.15	5.44	6.11	5.87	5.82	4.54	3.94	8.68	6.15	5.87	2.75	5.00	5.73	5.60	2.75	5.00	5.73	4.58	4.29	3.09	5.61	5.01	5.78	5.31	5.43	5.27
PbO	0.14	0.08	0.10	0.10	0.11	0.05	0.05	0.14	0.10	0.07	0.03	0.08	0.07	0.10	0.03	0.08	0.07	0.05	0.06	0.04	0.09	0.06	0.07	0.07	0.07	0.06
UO_2	0.96	0.17	0.25	0.43	0.40	0.12	0.09	0.47	0.20	0.37	0.18	0.18	0.18	1.30	0.18	0.18	0.18	0.10	0.56	0.16	0.17	0.16	0.18	0.34	0.30	0.18
Y_2O_3	1.16	0.57	1.44	2.01	1.96	0.49	0.48	2.23	0.98	3.40	1.15	0.96	1.42	3.00	1.15	0.96	1.42	0.52	3.87	0.91	0.72	1.27	1.42	1.62	2.48	1.02
La_2O_3	14.91	14.33	11.86	11.04	11.39	17.21	17.80	12.08	14.54	11.35	14.69	15.77	13.60	11.04	14.69	15.77	13.60	17.35	11.13	14.45	15.99	14.15	13.62	13.59	13.02	15.20
Ce_2O_3	28.15	29.61	27.47	27.48	27.76	30.68	30.87	26.26	29.12	26.46	30.46	30.10	28.87	26.53	30.46	30.10	28.87	30.70	26.61	30.10	30.02	29.37	28.90	29.04	27.95	29.96
Pr_2O_3	3.11	3.44	3.37	3.40	3.48	3.17	3.24	3.15	3.29	3.30	3.56	3.30	3.34	3.29	3.56	3.30	3.34	3.23	3.33	3.44	3.20	3.35	3.32	3.32	3.34	3.29
Nd_2O_3	11.34	12.73	12.52	12.96	13.16	11.73	11.43	11.57	11.67	12.56	13.24	11.80	12.50	12.35	13.24	11.80	12.50	11.83	12.61	13.43	11.55	12.64	12.49	12.74	12.53	11.92
Sm_2O_3	2.17	2.08	2.92	2.83	2.75	1.57	1.57	2.64	2.03	2.96	2.32	1.91	2.46	3.16	2.32	1.91	2.46	1.60	3.10	2.30	1.80	2.26	2.28	2.44	2.45	1.90
Eu_2O_3	0.08	0.02	0.01	0.11	0.17	0.03	0.03	0.12	0.10	bdl.	0.05	0.03	0.03	bdl.	0.05	0.03	0.03	bdl.	0.01	0.03	0.03	bdl.	0.01	0.00	0.03	0.01
Gd_2O_3	1.20	0.83	1.67	1.60	1.17	0.57	0.52	1.41	0.91	1.91	1.08	0.94	1.31	1.90	1.08	0.94	1.31	0.37	1.82	0.87	0.52	0.92	1.01	0.97	1.25	0.60
Tb_2O_3	0.06	0.08	0.16	0.16	0.13	0.04	0.08	0.18	0.10	0.22	0.05	0.02	0.06	0.24	0.05	0.02	0.06	0.07	0.21	0.09	0.09	0.06	0.09	0.14	0.16	0.06
Dy_2O_3	0.47	0.19	0.49	0.64	0.61	0.20	0.18	0.65	0.31	0.97	0.31	0.30	0.41	0.94	0.31	0.30	0.41	0.10	1.12	0.37	0.24	0.40	0.45	0.53	0.69	0.40
Ho_2O_3	0.06	0.02	0.03	0.05	0.02	bdl.	bdl.	0.08	0.03	0.08	0.01	0.01	0.04	0.09	0.01	0.01	0.04	bdl.	0.13	0.01	0.02	0.03	0.05	0.06	0.10	0.06
Er_2O_3	0.36	0.33	0.40	0.45	0.41	0.33	0.30	0.38	0.32	0.48	0.35	0.36	0.35	0.48	0.35	0.36	0.35	0.26	0.54	0.35	0.32	0.40	0.35	0.41	0.47	0.40
Tm_2O_3	0.05	0.04	0.06	0.06	0.06	0.07	0.03	0.05	0.06	0.08	0.04	0.07	0.05	0.05	0.04	0.07	0.05	0.03	0.08	0.05	0.06	0.05	0.07	0.07	0.09	0.05
Yb_2O_3	0.14	0.12	0.12	0.16	0.11	0.09	0.09	0.15	0.09	0.19	0.10	0.14	0.16	0.19	0.10	0.14	0.16	0.10	0.18	0.13	0.12	0.11	0.12	0.12	0.13	0.14
Lu_2O_3	0.07	0.12	0.13	0.06	0.12	0.10	0.09	0.06	0.10	0.05	0.14	0.07	0.01	0.09	0.14	0.07	0.01	0.06	0.09	0.09	0.08	0.10	0.08	0.16	0.09	0.05
FeO	bdl.	bdl.	0.01	bdl.	bdl.	bdl.	bdl.	bdl.	bdl.	0.01	0.02	bdl.	0.00	0.05	0.02	bdl.	0.00	bdl.	bdl.	0.02	bdl.	bdl.	0.00	0.08	0.05	0.22
SO_3	0.03	0.02	0.03	0.43	0.37	0.02	0.04	0.09	0.35	0.02	0.02	0.04	0.03	0.01	0.02	0.04	0.03	0.03	0.03	0.02	0.03	0.02	0.04	0.02	0.02	0.02
CaO	1.36	1.07	1.17	1.45	1.40	0.47	0.47	1.14	1.11	1.17	0.61	0.69	0.89	1.26	0.61	0.69	0.89	0.50	1.03	0.67	0.70	0.76	0.88	0.69	0.81	0.48
SrO	0.00	0.02	0.01	0.03	0.03	bdl.	0.02	0.02	bdl.	0.04	0.00	0.02	0.01	bdl.	0.00	0.02	0.01	0.00	0.01	0.03	0.02	0.01	bdl.	0.01	0.01	0.00
Al_2O_3	bdl.	bdl.	0.00	bdl.	bdl.	bdl.	bdl.	bdl.	bdl.	bdl.	bdl.	bdl.	bdl.	bdl.	bdl.	bdl.	bdl.	bdl.	bdl.	bdl.	bdl.	bdl.	bdl.	bdl.	bdl.	bdl.
Total	102.60	101.13	100.06	101.06	101.27	100.99	100.77	100.99	100.90	102.31	101.71	102.02	101.64	102.10	101.71	102.02	101.64	101.41	100.96	100.65	101.59	101.19	101.34	101.91	101.65	101.30
P	3.904	3.880	3.892	3.822	3.839	3.828	3.834	3.766	3.775	3.912	3.947	3.876	3.878	3.898	3.947	3.876	3.878	3.848	3.914	3.931	3.866	3.889	3.875	3.854	3.869	3.834
Si	0.071	0.070	0.072	0.088	0.076	0.121	0.107	0.179	0.136	0.059	0.031	0.091	0.085	0.061	0.031	0.091	0.085	0.118	0.035	0.033	0.114	0.079	0.097	0.112	0.093	0.145
As	0.010	0.013	0.012	0.011	0.012	0.012	0.012	0.011	0.012	0.011	0.011	0.012	0.011	0.011	0.011	0.012	0.011	0.012	0.011	0.012	0.012	0.011	0.012	0.012	0.011	0.012
Th	0.215	0.194	0.220	0.208	0.206	0.163	0.142	0.312	0.220	0.204	0.097	0.177	0.203	0.196	0.097	0.177	0.203	0.163	0.151	0.110	0.199	0.178	0.205	0.188	0.192	0.188
U	0.033	0.006	0.009	0.015	0.014	0.004	0.003	0.016	0.007	0.013	0.006	0.006	0.006	0.045	0.006	0.006	0.006	0.004	0.019	0.006	0.006	0.005	0.006	0.012	0.010	0.006
Pb	0.006	0.004	0.004	0.004	0.004	0.002	0.002	0.006	0.004	0.003	0.001	0.003	0.003	0.004	0.001	0.003	0.003	0.002	0.002	0.002	0.004	0.003	0.003	0.003	0.003	0.003
Y	0.095	0.047	0.121	0.167	0.162	0.041	0.041	0.187	0.082	0.277	0.095	0.079	0.118	0.246	0.095	0.079	0.118	0.044	0.320	0.076	0.060	0.106	0.117	0.134	0.205	0.085
La	0.845	0.829	0.691	0.634	0.652	1.004	1.039	0.703	0.843	0.640	0.837	0.903	0.781	0.627	0.837	0.903	0.781	1.002	0.637	0.835	0.919	0.815	0.783	0.779	0.745	0.878
Ce	1.583	1.701	1.588	1.565	1.578	1.776	1.789	1.517	1.677	1.481	1.722	1.710	1.645	1.496	1.722	1.710	1.645	1.761	1.511	1.726	1.713	1.679	1.649	1.653	1.588	1.717
Pr	0.174	0.197	0.194	0.193	0.197	0.182	0.187	0.181	0.189	0.184	0.200	0.186	0.190	0.185	0.200	0.186	0.190	0.184	0.188	0.196	0.182	0.191	0.188	0.188	0.189	0.188
Nd	0.622	0.714	0.706	0.720	0.729	0.662	0.646	0.652	0.656	0.686	0.730	0.654	0.695	0.679	0.730	0.654	0.695	0.662	0.698	0.751	0.643	0.705	0.696	0.708	0.694	0.666
Sm	0.115	0.113	0.159	0.152	0.147	0.086	0.086	0.144	0.110	0.156	0.124	0.102	0.132	0.168	0.124	0.102	0.132	0.087	0.166	0.124	0.097	0.122	0.123	0.131	0.131	0.103
Eu	0.004	0.001	0.000	0.006	0.009	0.002	0.002	0.006	0.005	0.000	0.002	0.002	0.001	0.000	0.002	0.002	0.001	0.000	0.000	0.002	0.002	0.000	0.001	0.000	0.002	0.001
Gd	0.061	0.043	0.087	0.082	0.060	0.030	0.027	0.074	0.047	0.097	0.055	0.048	0.068	0.097	0.055	0.048	0.068	0.019	0.093	0.045	0.027	0.047	0.052	0.050	0.064	0.031
Tb	0.003	0.004	0.008	0.008	0.007	0.002	0.004	0.009	0.005	0.011	0.002	0.001	0.003	0.012	0.002	0.001	0.003	0.004	0.011	0.005	0.005	0.003	0.004	0.007	0.008	0.003
Dy	0.023	0.010	0.025	0.032	0.030	0.010	0.009	0.033	0.016	0.048	0.015	0.015	0.021	0.047	0.015	0.015	0.021	0.005	0.056	0.019	0.012	0.020	0.023	0.027	0.035	0.020
Ho	0.003	0.001	0.002	0.003	0.001	0.000	0.000	0.004	0.002	0.004	0.000	0.000	0.002	0.004	0.000	0.000	0.002	0.000	0.006	0.000	0.001	0.002	0.002	0.003	0.005	0.003
Er	0.017	0.016	0.020	0.022	0.020	0.016	0.015	0.019	0.016	0.023	0.017	0.018	0.017	0.023	0.017	0.018	0.017	0.013	0.026	0.017	0.016	0.020	0.017	0.020	0.023	0.019
Tm	0.002	0.002	0.003	0.003	0.003	0.003	0.002	0.002	0.003	0.004	0.002	0.003	0.003	0.003	0.002	0.003	0.003	0.001	0.004	0.002	0.003	0.003	0.003	0.003	0.004	0.003
Yb	0.007	0.006	0.006	0.007	0.005	0.005	0.004	0.007	0.004	0.009	0.005	0.007	0.007	0.009	0.005	0.007	0.007	0.005	0.009	0.006	0.006	0.005	0.006	0.006	0.006	0.007
Lu	0.003	0.006	0.006	0.003	0.005	0.005	0.004	0.003	0.005	0.002	0.007	0.003	0.001	0.004	0.007	0.003	0.001	0.003	0.004	0.004	0.004	0.005	0.004	0.007	0.004	0.002
Fe^{2+}	0.000	0.000	0.001	0.000	0.000	0.000	0.000	0.000	0.000	0.002	0.002	0.000	0.000	0.006	0.002	0.000	0.000	0.000	0.000	0.002	0.000	0.000	0.000	0.011	0.006	0.029
S	0.003	0.003	0.004	0.051	0.044	0.003	0.005	0.011	0.041	0.003	0.003	0.005	0.003	0.001	0.003	0.005	0.003	0.003	0.003	0.002	0.004	0.003	0.004	0.002	0.003	0.002
Ca	0.224	0.180	0.198	0.242	0.233	0.080	0.080	0.192	0.186	0.191	0.101	0.116	0.149	0.207	0.101	0.116	0.149	0.083	0.170	0.113	0.116	0.128	0.147	0.115	0.135	0.081
Sr	0.000	0.002	0.001	0.003	0.003	0.000	0.001	0.001	0.000	0.003	0.000	0.002	0.001	0.000	0.000	0.002	0.001	0.000	0.001	0.003	0.002	0.001	0.000	0.001	0.001	0.000
Al	0.000	0.000	0.000	0.000	0.000	0.000	0.000	0.000	0.000	0.000	0.000	0.000	0.000	0.000	0.000	0.000	0.000	0.000	0.000	0.000	0.000	0.000	0.000	0.000	0.000	0.000
Σcat.	8.024	8.040	8.028	8.040	8.037	8.036	8.041	8.035	8.042	8.023	8.015	8.019	8.023	8.031	8.015	8.019	8.023	8.023	8.036	8.025	8.012	8.020	8.018	8.026	8.027	8.025
Age (Ma)	353	344	340	348	358	266	272	340	346	247	247	352	271	255	247	352	271	257	236	255	371	274	262	261	253	252
2 sd	17.4	26.3	22.7	21.9	22.5	30.8	35.2	16.3	23.5	21.7	44.1	28.2	24.4	15.8	44.1	28.2	24.4	30.3	24.2	40.2	25.8	27.2	23.8	23.5	23.5	25.7

Electronic supplement

VOZÁROVÁ et al.: Provenance of Permian Malužiná Formation sandstones (Hronicum, Western Carpathians): evidence from monazite geochronology

Appendix 1

Table 3: *Continued.*

Sample	23-VD																														
Point	**1/1 C.**	**1/2 C.**	**1/3 C.**	**2/1 C.**	**2/2 C.**	**3/1 C.**	**3/2 C.**	**3/3 C.**	**4/1 C.**	**4/2 C.**	**4/3 C.**	**4/4 C.**	**4/5 C.**	**4/6 C.**	**4/7 C.**	**5/1 C.**	**5/2 C.**	**5/3 C.**	**5/4 C.**	**5/5 C.**	**5/6 C.**	**5/7 C.**	**5/8 C.**	**5/9 C.**	**6/1 C.**	**6/2 C.**	**6/3 C.**	**6/4 C.**	**6/5 C.**	**7/1 C.**	**7/2 C.**	**7/3 C.**
P_2O_5	28.73	28.98	29.03	30.85	30.81	29.85	29.85	30.12	30.09	30.12	30.08	29.89	29.92	29.65	29.82	27.16	30.34	30.31	28.85	28.84	30.03	29.94	27.84	27.64	30.67	30.90	31.04	30.98	31.04	31.38	31.33	30.65
As_2O_5	0.15	0.14	0.14	0.13	0.13	0.14	0.15	0.14	0.13	0.13	0.14	0.14	0.14	0.12	0.14	0.14	0.13	0.14	0.14	0.14	0.14	0.14	0.13	0.14	0.13	0.14	0.14	0.13	0.13	0.13	0.12	0.14
SiO_2	0.66	0.65	0.75	0.35	0.36	0.25	0.26	0.26	0.18	0.22	0.28	0.26	0.26	0.32	0.30	1.86	0.18	0.17	0.86	0.87	0.19	0.18	1.53	1.84	0.20	0.15	0.15	0.23	0.16	0.22	0.24	0.34
ThO_2	6.07	7.18	6.81	4.61	4.43	3.89	3.73	3.07	3.43	3.50	3.97	3.16	3.42	4.18	3.66	10.19	4.82	4.88	5.80	5.78	4.81	5.07	9.76	9.91	3.76	3.88	3.96	3.74	3.86	3.72	3.78	3.96
PbO	0.10	0.11	0.11	0.11	0.10	0.10	0.10	0.08	0.09	0.09	0.10	0.08	0.09	0.12	0.11	0.16	0.13	0.13	0.10	0.10	0.19	0.14	0.15	0.18	0.08	0.08	0.08	0.09	0.08	0.12	0.11	0.12
UO_2	0.16	0.22	0.18	0.81	0.71	0.86	0.83	0.70	0.81	0.78	0.94	0.79	0.82	1.02	1.09	0.35	1.28	1.25	0.32	0.34	2.43	1.39	0.39	0.74	0.53	0.51	0.55	0.55	0.52	1.31	1.15	1.28
Y_2O_3	0.44	0.90	0.42	2.26	2.00	0.86	0.76	0.89	1.95	1.76	0.84	0.67	0.69	0.80	0.77	1.20	2.37	2.61	1.39	1.42	2.23	2.44	1.65	1.65	2.73	2.88	2.96	2.69	2.81	2.84	2.66	1.31
La_2O_3	14.85	12.89	14.21	13.54	13.60	13.42	13.64	13.83	12.68	12.79	13.08	13.71	13.25	12.94	13.07	12.11	13.07	12.53	13.18	12.96	13.21	12.99	12.01	12.16	12.28	12.24	12.09	12.20	12.51	13.32	13.56	14.26
Ce_2O_3	30.17	29.15	30.03	28.49	28.76	28.77	29.32	29.54	27.60	28.04	28.70	29.18	28.75	28.11	28.69	26.28	27.90	27.11	28.61	28.29	27.72	27.36	26.06	25.79	27.06	27.03	27.04	27.55	27.10	27.53	27.76	28.63
Pr_2O_3	3.34	3.33	3.40	3.26	3.30	3.54	3.41	3.45	3.34	3.34	3.55	3.43	3.46	3.33	3.34	3.17	3.22	3.21	3.39	3.31	3.13	3.16	3.17	3.17	3.35	3.36	3.34	3.38	3.37	3.24	3.23	3.37
Nd_2O_3	12.09	12.50	11.84	12.27	12.22	13.45	13.28	13.57	13.35	13.33	13.45	13.66	13.79	13.46	13.52	12.47	11.94	12.23	12.82	12.66	11.40	11.88	12.42	12.26	13.35	13.41	13.28	13.34	13.56	11.97	12.01	12.51
Sm_2O_3	1.62	2.01	1.55	2.08	2.12	2.48	2.41	2.47	2.70	2.72	2.69	2.65	2.64	2.67	2.72	2.38	2.15	2.28	2.32	2.33	1.87	2.14	2.52	2.18	2.72	2.80	2.81	2.83	2.80	2.37	2.32	2.25
Eu_2O_3	bdl.	bdl.	bdl.	bdl.	bdl.	bdl.	bdl.	bdl.	bdl.	bdl.	bdl.	bdl.	bdl.	bdl.	bdl.	bdl.	bdl.	bdl.	bdl.	bdl.	bdl.	bdl.	bdl.	bdl.	bdl.	bdl.	bdl.	bdl.	bdl.	bdl.	bdl.	bdl.
Gd_2O_3	0.97	1.17	0.86	1.48	1.45	1.88	1.80	1.86	2.36	2.19	1.87	1.94	1.90	1.98	1.90	1.63	1.59	1.74	1.59	1.61	1.36	1.63	1.77	1.55	2.14	2.19	2.29	2.13	2.23	1.93	1.92	1.53
Tb_2O_3	0.00	0.08	0.01	0.14	0.11	0.09	0.11	0.12	0.20	0.19	0.13	0.12	0.12	0.19	0.08	0.08	0.15	0.17	0.11	0.10	0.11	0.14	0.10	0.12	0.16	0.17	0.24	0.20	0.14	0.14	0.22	0.08
Dy_2O_3	0.16	0.25	0.15	0.62	0.60	0.41	0.39	0.48	0.85	0.77	0.47	0.36	0.39	0.42	0.42	0.42	0.66	0.79	0.41	0.47	0.52	0.67	0.51	0.47	0.87	0.90	0.92	0.85	0.92	0.83	0.90	0.48
Ho_2O_3	0.02	0.06	0.01	0.06	0.07	0.00	0.05	0.00	0.07	0.08	0.03	0.06	bdl.	0.02	0.04	0.04	0.01	0.08	0.01	0.11	0.09	0.07	0.07	0.03	0.09	0.04	0.08	0.07	0.05	0.02	0.06	0.02
Er_2O_3	0.36	0.35	0.31	0.47	0.47	0.38	0.30	0.31	0.41	0.41	0.34	0.31	0.38	0.36	0.33	0.41	0.43	0.51	0.43	0.37	0.45	0.45	0.43	0.44	0.47	0.50	0.46	0.45	0.48	0.52	0.45	0.36
Tm_2O_3	0.06	0.09	0.11	0.06	0.09	0.07	0.07	0.06	0.08	0.08	0.11	0.06	0.05	0.06	0.09	0.10	0.08	0.08	0.09	0.06	0.11	0.10	0.08	0.08	0.15	0.11	0.07	0.06	0.08	0.04	0.09	0.09
Yb_2O_3	0.14	0.11	0.12	0.19	0.17	0.09	0.10	0.13	0.09	0.11	0.15	0.08	0.12	0.09	0.14	0.11	0.14	0.18	0.14	0.15	0.12	0.13	0.16	0.13	0.15	0.11	0.17	0.14	0.15	0.18	0.16	0.14
Lu_2O_3	bdl.	bdl.	bdl.	bdl.	bdl.	bdl.	bdl.	bdl.	bdl.	bdl.	bdl.	bdl.	bdl.	bdl.	bdl.	bdl.	bdl.	bdl.	bdl.	bdl.	bdl.	bdl.	bdl.	bdl.	bdl.	bdl.	bdl.	bdl.	bdl.	bdl.	bdl.	bdl.
FeO	0.06	0.05	0.02	0.14	0.22	0.05	0.14	0.12	0.07	0.03	bdl.	bdl.	bdl.	0.00	0.05	0.06	bdl.	0.01	bdl.	bdl.	0.08	bdl.	bdl.	0.11	0.30	0.13	0.14	0.14	0.11	0.17	0.13	0.14
SO_3	0.02	0.06	0.03	0.02	0.05	0.03	0.03	0.02	0.01	0.01	0.03	0.02	0.02	0.02	0.02	0.19	0.01	0.02	0.26	0.23	0.02	0.01	0.17	0.13	0.04	0.02	0.02	0.03	0.03	0.03	0.02	0.03
CaO	0.87	1.18	0.99	0.96	0.94	0.96	0.88	0.74	0.87	0.86	0.96	0.75	0.80	0.98	0.88	0.92	1.28	1.27	0.92	0.90	1.48	1.33	1.05	1.00	0.94	0.90	0.93	0.89	0.91	1.02	0.99	0.99
SrO	0.03	0.02	0.01	0.02	0.07	0.01	0.00	0.01	0.01	0.03	0.02	0.02	0.00	bdl.	0.01	0.03	0.01	0.01	0.04	0.03	0.01	0.01	0.03	0.03	0.02	0.03	0.03	0.02	0.01	0.04	0.01	0.02
Al_2O_3	bdl.	bdl.	bdl.	bdl.	bdl.	bdl.	bdl.	bdl.	bdl.	bdl.	bdl.	bdl.	bdl.	bdl.	bdl.	bdl.	bdl.	bdl.	bdl.	bdl.	bdl.	bdl.	bdl.	bdl.	0.03	bdl.	bdl.	0.01	bdl.	0.00	bdl.	0.04
Total	101.06	101.49	101.09	102.93	102.77	101.58	101.60	101.98	101.36	101.58	101.93	101.34	100.99	100.86	101.20	101.47	101.90	101.70	101.76	101.06	101.71	101.37	102.00	101.74	102.23	102.48	102.79	102.71	103.04	103.07	103.21	102.76
P	3.840	3.844	3.858	3.953	3.953	3.927	3.926	3.938	3.946	3.944	3.937	3.940	3.949	3.929	3.935	3.649	3.945	3.947	3.803	3.818	3.926	3.929	3.704	3.680	3.954	3.971	3.974	3.969	3.970	3.987	3.983	3.948
Si	0.104	0.102	0.117	0.054	0.054	0.040	0.040	0.040	0.028	0.034	0.043	0.040	0.040	0.050	0.046	0.296	0.027	0.026	0.134	0.136	0.030	0.028	0.240	0.289	0.030	0.022	0.023	0.034	0.024	0.033	0.036	0.052
As	0.012	0.012	0.012	0.010	0.010	0.011	0.012	0.012	0.011	0.010	0.011	0.012	0.011	0.010	0.011	0.011	0.010	0.011	0.012	0.011	0.012	0.011	0.011	0.012	0.010	0.011	0.011	0.010	0.010	0.010	0.010	0.011
Th	0.218	0.256	0.243	0.159	0.153	0.138	0.132	0.108	0.121	0.123	0.140	0.112	0.121	0.149	0.130	0.368	0.169	0.171	0.205	0.206	0.169	0.179	0.349	0.355	0.130	0.134	0.136	0.129	0.133	0.127	0.129	0.137
U	0.006	0.008	0.006	0.027	0.024	0.030	0.029	0.024	0.028	0.027	0.032	0.027	0.028	0.036	0.038	0.012	0.044	0.043	0.011	0.012	0.083	0.048	0.014	0.026	0.018	0.017	0.019	0.019	0.018	0.044	0.039	0.043
Pb	0.004	0.005	0.005	0.004	0.004	0.004	0.004	0.003	0.004	0.004	0.004	0.003	0.004	0.005	0.005	0.007	0.005	0.005	0.004	0.004	0.008	0.006	0.006	0.008	0.003	0.003	0.003	0.003	0.003	0.005	0.004	0.005
Y	0.037	0.075	0.035	0.182	0.162	0.071	0.063	0.073	0.160	0.145	0.069	0.055	0.057	0.067	0.064	0.101	0.194	0.214	0.115	0.118	0.183	0.201	0.138	0.138	0.221	0.233	0.239	0.217	0.226	0.227	0.213	0.106
La	0.865	0.745	0.822	0.756	0.760	0.769	0.782	0.788	0.724	0.730	0.746	0.787	0.762	0.747	0.751	0.709	0.741	0.711	0.757	0.747	0.753	0.743	0.696	0.705	0.690	0.686	0.675	0.681	0.697	0.737	0.751	0.800
Ce	1.744	1.672	1.725	1.579	1.595	1.637	1.668	1.670	1.565	1.588	1.625	1.663	1.641	1.611	1.637	1.527	1.569	1.527	1.631	1.620	1.567	1.553	1.500	1.485	1.509	1.502	1.497	1.526	1.498	1.513	1.526	1.595
Pr	0.192	0.190	0.195	0.180	0.182	0.201	0.193	0.194	0.189	0.188	0.200	0.194	0.196	0.190	0.190	0.183	0.180	0.180	0.192	0.189	0.176	0.179	0.181	0.182	0.186	0.186	0.184	0.187	0.185	0.177	0.176	0.187
Nd	0.682	0.700	0.664	0.663	0.661	0.747	0.737	0.749	0.739	0.736	0.743	0.760	0.768	0.752	0.753	0.707	0.655	0.671	0.713	0.707	0.629	0.658	0.697	0.688	0.726	0.727	0.717	0.721	0.731	0.641	0.644	0.680
Sm	0.088	0.109	0.084	0.109	0.111	0.133	0.129	0.132	0.145	0.145	0.144	0.142	0.142	0.144	0.147	0.131	0.114	0.121	0.125	0.126	0.100	0.115	0.137	0.118	0.143	0.147	0.147	0.148	0.146	0.123	0.120	0.118
Eu	0.000	0.000	0.000	0.000	0.000	0.000	0.000	0.000	0.000	0.000	0.000	0.000	0.000	0.000	0.000	0.000	0.000	0.000	0.000	0.000	0.000	0.000	0.000	0.000	0.000	0.000	0.000	0.000	0.000	0.000	0.000	0.000
Gd	0.051	0.061	0.045	0.074	0.073	0.097	0.093	0.095	0.121	0.112	0.096	0.100	0.098	0.103	0.098	0.086	0.081	0.089	0.082	0.083	0.070	0.084	0.092	0.081	0.108	0.110	0.115	0.107	0.112	0.096	0.096	0.077
Tb	0.000	0.004	0.001	0.007	0.006	0.005	0.005	0.006	0.010	0.010	0.007	0.006	0.006	0.010	0.004	0.004	0.007	0.009	0.005	0.005	0.006	0.007	0.005	0.006	0.008	0.009	0.012	0.010	0.007	0.007	0.011	0.004
Dy	0.008	0.013	0.007	0.030	0.029	0.021	0.019	0.024	0.042	0.039	0.023	0.018	0.019	0.021	0.021	0.022	0.033	0.039	0.021	0.024	0.026	0.033	0.026	0.024	0.043	0.044	0.045	0.042	0.045	0.040	0.044	0.024
Ho	0.001	0.003	0.001	0.003	0.003	0.000	0.003	0.000	0.003	0.004	0.001	0.003	0.000	0.001	0.002	0.002	0.001	0.004	0.000	0.005	0.004	0.004	0.003	0.001	0.004	0.002	0.004	0.003	0.002	0.001	0.003	0.001
Er	0.018	0.017	0.015	0.022	0.022	0.018	0.015	0.015	0.020	0.020	0.017	0.015	0.019	0.017	0.016	0.021	0.021	0.025	0.021	0.018	0.022	0.022	0.021	0.022	0.022	0.024	0.022	0.022	0.023	0.025	0.021	0.017
Tm	0.003	0.004	0.006	0.003	0.004	0.004	0.003	0.003	0.004	0.004	0.005	0.003	0.003	0.003	0.004	0.005	0.004	0.004	0.004	0.003	0.005	0.005	0.004	0.004	0.007	0.005	0.003	0.003	0.004	0.002	0.004	0.004
Yb	0.007	0.005	0.006	0.009	0.008	0.004	0.005	0.006	0.004	0.005	0.007	0.004	0.006	0.004	0.007	0.005	0.007	0.008	0.007	0.007	0.006	0.006	0.008	0.006	0.007	0.005	0.008	0.007	0.007	0.008	0.007	0.007
Lu	0.000	0.000	0.000	0.000	0.000	0.000	0.000	0.000	0.000	0.000	0.000	0.000	0.000	0.000	0.000	0.000	0.000	0.000	0.000	0.000	0.000	0.000	0.000	0.000	0.000	0.000	0.000	0.000	0.000	0.000	0.000	0.000
Fe^{2+}	0.008	0.006	0.002	0.018	0.028	0.006	0.018	0.016	0.009	0.004	0.000	0.000	0.000	0.000	0.006	0.008	0.000	0.001	0.000	0.000	0.011	0.000	0.000	0.015	0.039	0.017	0.018	0.018	0.014	0.022	0.016	0.018
S	0.003	0.007	0.003	0.003	0.006	0.004	0.004	0.002	0.001	0.001	0.003	0.002	0.002	0.002	0.002	0.022	0.001	0.002	0.030	0.027	0.003	0.001	0.020	0.016	0.005	0.003	0.002	0.003	0.003	0.004	0.002	0.003
Ca	0.148	0.199	0.166	0.156	0.152	0.161	0.147	0.122	0.145	0.142	0.159	0.125	0.134	0.165	0.148	0.157	0.211	0.210	0.154	0.151	0.244	0.221	0.177	0.168	0.154	0.146	0.150	0.145	0.148	0.164	0.159	0.161
Sr	0.002	0.001	0.001	0.002	0.006	0.001	0.000	0.001	0.001	0.003	0.001	0.002	0.000	0.000	0.001	0.003	0.001	0.001	0.004	0.003	0.001	0.001	0.003	0.003	0.002	0.003	0.002	0.002	0.001	0.003	0.001	0.001
Al	0.000	0.000	0.000	0.000	0.000	0.000	0.000	0.000	0.000	0.000	0.000	0.000	0.000	0.000	0.000	0.000	0.000	0.000	0.000	0.000	0.000	0.000	0.000	0.000	0.005	0.000	0.000	0.001	0.000	0.000	0.000	0.008
Σcat.	8.040	8.037	8.019	8.002	8.005	8.026	8.027	8.021	8.021	8.019	8.014	8.014	8.007	8.017	8.016	8.036	8.020	8.018	8.030	8.021	8.032	8.030	8.032	8.031	8.025	8.007	8.006	8.006	8.007	7.995	7.995	8.009
Age (Ma)	**355**	**347**	**369**	**352**	**369**	**360**	**365**	**351**	**344**	**340**	**353**	**345**	**364**	**365**	**355**	**348**	**351**	**341**	**363**	**349**	**345**	**351**	**331**	**352**	**345**	**349**	**342**	**368**	**342**	**351**	**349**	**343**
2 sd	25.8	21.8	23.4	23.9	25.5	25.3	25.9	30.9	27.3	27.4	24.0	28.8	27.3	22.6	23.4	16.0	19.1	19.3	25.2	24.8	14.1	18.1	16.1	14.9	30.7	30.1	29.2	30.5	30.0	21.5	22.8	20.9

Electronic supplement

VOZÁROVÁ et al.: Provenance of Permian Malužiná Formation sandstones (Hronicum, Western Carpathians): evidence from monazite geochronology

Appendix 1

Table 3: *Continued.*

Sample	31-VD						32-VD		33-VD		22-VD						
Point	1/1 C.	1/2 C.	2/1 C.	2/2 C.	3/1 C.	3/2 C.	1/1 C.	2/1 C.	1/1 C.	2/1 C.	2/1 C.	2/2 C.	2/3 C.	4/1 P.	4/4 P.	4/5 P.	5/1 P.
P_2O_5	31.08	29.92	30.26	29.94	29.74	29.78	29.94	29.74	29.32	29.54	29.96	30.21	30.19	29.12	29.01	28.45	28.20
As_2O_5	0.08	0.09	0.08	0.09	0.09	0.09	0.10	0.09	0.08	0.09	0.13	0.14	0.13	0.32	0.49	0.64	0.51
SiO_2	0.29	0.37	0.23	0.26	0.43	0.43	0.41	0.50	0.40	0.44	0.28	0.25	0.20	0.81	0.74	0.55	0.40
ThO_2	2.70	4.04	2.54	3.22	3.86	3.86	4.05	6.57	5.08	2.11	3.27	3.41	3.60	6.50	3.72	3.67	2.59
PbO	0.06	0.08	0.06	0.09	0.06	0.06	0.07	0.12	0.10	0.07	0.09	0.09	0.10	0.07	0.04	0.04	0.04
UO_2	0.57	0.68	0.52	0.58	0.32	0.31	0.29	0.42	0.68	0.68	0.93	0.90	0.84	0.11	0.05	0.07	0.37
Y_2O_3	1.70	1.10	1.83	1.77	1.83	1.85	1.28	1.55	1.88	0.69	2.37	2.07	1.84	0.25	0.18	0.19	0.98
La_2O_3	13.55	13.75	13.35	13.05	13.43	13.57	14.93	12.25	12.12	13.52	12.57	12.76	12.88	15.08	17.07	16.59	14.65
Ce_2O_3	28.67	29.12	28.27	27.61	28.69	28.71	29.70	27.65	27.09	29.64	27.66	27.81	28.33	31.43	32.69	32.65	29.12
Pr_2O_3	3.46	3.36	3.47	3.28	3.38	3.41	3.30	3.39	3.32	3.63	3.34	3.35	3.51	3.22	3.26	3.19	3.26
Nd_2O_3	13.50	13.10	14.09	13.73	12.91	12.85	12.51	12.94	13.44	14.38	13.31	13.38	13.29	10.31	11.03	10.31	11.80
Sm_2O_3	2.51	2.28	2.92	2.87	2.54	2.57	1.87	2.36	2.86	2.76	2.93	2.93	2.88	1.50	1.53	1.53	2.32
Eu_2O_3	bdl.	bdl.	bdl.	bdl.	bdl.	bdl.	bdl.	bdl.	bdl.	bdl.	0.16	0.12	0.11	0.37	0.37	0.43	0.26
Gd_2O_3	1.87	1.69	2.10	2.20	1.94	1.83	1.24	1.62	2.05	2.06	2.09	1.97	1.80	0.32	0.31	0.32	1.02
Tb_2O_3	0.16	0.14	0.19	0.14	0.12	0.17	0.07	0.11	0.24	0.10	0.25	0.21	0.17	0.05	0.05	0.02	0.10
Dy_2O_3	0.64	0.37	0.71	0.71	0.67	0.71	0.38	0.42	0.69	0.34	1.01	0.86	0.83	0.05	0.13	0.12	0.42
Ho_2O_3	0.05	0.04	0.12	0.10	0.04	0.05	0.03	0.03	0.06	0.01	0.07	0.10	0.07	bdl.	bdl.	0.01	0.07
Er_2O_3	0.43	0.30	0.43	0.40	0.37	0.42	0.35	0.40	0.45	0.31	0.37	0.34	0.30	0.33	0.30	0.26	0.32
Tm_2O_3	0.07	0.13	0.08	0.10	0.09	0.09	0.06	0.10	0.09	0.09	0.04	0.04	0.02	0.06	0.04	0.03	0.04
Yb_2O_3	0.10	0.11	0.15	0.15	0.10	0.17	0.11	0.12	0.14	0.13	0.10	0.13	0.13	0.11	0.12	0.09	0.09
Lu_2O_3	bdl.	bdl.	bdl.	bdl.	bdl.	bdl.	bdl.	bdl.	bdl.	bdl.	0.07	0.05	0.05	0.07	0.06	0.04	0.13
FeO	0.06	0.10	0.28	0.44	0.33	0.38	bdl.	bdl.	0.07	0.30	bdl.	bdl.	bdl.	0.17	0.52	0.51	0.07
SO_3	0.02	0.03	0.03	0.04	0.02	0.02	0.03	0.00	0.02	0.02	0.02	0.03	0.03	0.23	0.18	0.15	0.09
CaO	0.60	0.96	0.71	0.79	0.64	0.63	1.03	1.39	1.10	0.59	0.76	0.85	0.90	1.13	0.63	0.71	0.62
SrO	0.00	0.03	0.03	0.02	0.00	bdl.	0.01	0.00	bdl.	0.01	0.00	0.01	0.01	0.40	0.22	0.25	0.06
Al_2O_3	0.00	bdl.	0.00	0.00	bdl.	bdl.	bdl.	bdl.	0.02	bdl.	bdl.	bdl.	bdl.	bdl.	0.01	bdl.	0.00
Total	102.18	101.81	102.46	101.58	101.62	101.97	101.76	101.75	101.30	101.52	101.79	102.02	102.20	102.01	102.75	100.83	97.53
P	3.996	3.918	3.931	3.924	3.904	3.899	3.913	3.899	3.882	3.898	3.921	3.937	3.935	3.818	3.793	3.796	3.865
Si	0.044	0.058	0.035	0.040	0.067	0.067	0.063	0.077	0.062	0.068	0.044	0.039	0.031	0.125	0.114	0.087	0.064
As	0.006	0.007	0.007	0.007	0.007	0.008	0.008	0.007	0.006	0.008	0.010	0.011	0.011	0.026	0.040	0.053	0.043
Th	0.093	0.142	0.089	0.113	0.136	0.136	0.142	0.231	0.181	0.075	0.115	0.119	0.126	0.229	0.131	0.132	0.095
U	0.019	0.023	0.018	0.020	0.011	0.011	0.010	0.014	0.024	0.023	0.032	0.031	0.029	0.004	0.002	0.002	0.013
Pb	0.002	0.003	0.003	0.004	0.003	0.003	0.003	0.005	0.004	0.003	0.004	0.004	0.004	0.003	0.002	0.002	0.002
Y	0.137	0.091	0.150	0.145	0.151	0.152	0.105	0.127	0.156	0.057	0.195	0.169	0.151	0.020	0.015	0.016	0.084
La	0.759	0.785	0.755	0.745	0.768	0.774	0.850	0.699	0.699	0.777	0.717	0.724	0.731	0.862	0.972	0.964	0.875
Ce	1.594	1.649	1.588	1.565	1.628	1.626	1.678	1.567	1.551	1.691	1.565	1.567	1.596	1.782	1.848	1.884	1.726
Pr	0.191	0.190	0.194	0.185	0.191	0.192	0.185	0.191	0.189	0.206	0.188	0.188	0.197	0.182	0.183	0.183	0.192
Nd	0.732	0.724	0.772	0.759	0.715	0.710	0.690	0.715	0.750	0.800	0.735	0.736	0.730	0.570	0.608	0.580	0.682
Sm	0.131	0.122	0.155	0.153	0.136	0.137	0.100	0.126	0.154	0.149	0.157	0.156	0.153	0.080	0.081	0.083	0.130
Eu	0.000	0.000	0.000	0.000	0.000	0.000	0.000	0.000	0.000	0.000	0.008	0.006	0.006	0.020	0.020	0.023	0.015
Gd	0.094	0.087	0.107	0.113	0.100	0.094	0.063	0.083	0.106	0.106	0.107	0.100	0.092	0.016	0.016	0.017	0.055
Tb	0.008	0.007	0.010	0.007	0.006	0.009	0.004	0.006	0.012	0.005	0.013	0.011	0.009	0.003	0.002	0.001	0.005
Dy	0.032	0.018	0.035	0.036	0.034	0.035	0.019	0.021	0.035	0.017	0.050	0.043	0.041	0.003	0.006	0.006	0.022
Ho	0.003	0.002	0.006	0.005	0.002	0.002	0.001	0.001	0.003	0.001	0.003	0.005	0.003	0.000	0.000	0.000	0.004
Er	0.021	0.014	0.021	0.019	0.018	0.021	0.017	0.019	0.022	0.015	0.018	0.017	0.014	0.016	0.014	0.013	0.016
Tm	0.003	0.006	0.004	0.005	0.004	0.004	0.003	0.005	0.004	0.004	0.002	0.002	0.001	0.003	0.002	0.001	0.002
Yb	0.005	0.005	0.007	0.007	0.005	0.008	0.005	0.006	0.007	0.006	0.005	0.006	0.006	0.005	0.005	0.004	0.004
Lu	0.000	0.000	0.000	0.000	0.000	0.000	0.000	0.000	0.000	0.000	0.003	0.002	0.002	0.003	0.003	0.002	0.007
Fe^{2+}	0.008	0.013	0.037	0.057	0.043	0.049	0.000	0.000	0.009	0.039	0.000	0.000	0.000	0.022	0.068	0.067	0.009
S	0.002	0.004	0.004	0.005	0.002	0.002	0.004	0.000	0.002	0.003	0.003	0.003	0.003	0.027	0.021	0.018	0.010
Ca	0.098	0.159	0.116	0.130	0.106	0.105	0.171	0.230	0.185	0.098	0.126	0.140	0.149	0.188	0.104	0.119	0.108
Sr	0.000	0.003	0.003	0.001	0.000	0.000	0.001	0.000	0.000	0.001	0.000	0.001	0.001	0.036	0.020	0.023	0.006
Al	0.000	0.000	0.000	0.001	0.000	0.000	0.000	0.000	0.004	0.000	0.000	0.000	0.000	0.000	0.003	0.000	0.000
Σcat.	7.980	8.031	8.043	8.048	8.036	8.042	8.035	8.033	8.049	8.051	8.022	8.017	8.022	8.041	8.072	8.078	8.034
Age (Ma)	**311**	**323**	**345**	**401**	**315**	**319**	**358**	**365**	**332**	**391**	**345**	**355**	**359**	**246**	**229**	**254**	**256**
2 sd	35.4	26.8	38.3	32.9	33.8	33.6	33.5	22.0	31.4	37.9	24.3	24.6	24.7	21.8	37.2	37.2	38.5